NONPERTURBATIVE QUANTUM FIELD THEORY ON THE LATTICE

THOMAS DeGRAND
Department of Physics, University of Colorado, Boulder CO 80309-390

These lectures provide an introduction to lattice methods for nonperturbative studies of quantum field theories, with an emphasis on Quantum Chromodynamics. Lecture 1 (Ch. 2): gauge field basics; lecture 2 (Ch. 3): Abelian duality with a lattice regulator; (Ch. 4) simple lattice intuition; lecture 3 (Ch. 5): standard methods (and results) for hadron spectroscopy; lecture 4 (Ch. 6): bare actions and physics; lecture 5 (Ch. 7): two case studies, the mass of the glueball, and $\alpha_s(M_Z)$.

1 Introduction

The physics of the 20th century is the physics of local gauge invariance. Lattice gauge theories present an extreme limit, being systems with exact internal symmetries but no (or very restricted) space time symmetries. These lectures are intended to be an introduction to the lattice approach to quantum field theories in general and to QCD in particular [1]. The use of a lattice regulator is a standard technique for studying strong coupling when space-time symmetries can be regarded as secondary. Many techniques of lattice have found a home or at least a word in the vocabulary of string. Some of these techniques might be useful to you. Lattice methods have been used to study random surfaces in the context of models for quantum gravity, but I will not discuss that subject here.

Lattice gauge theory was invented by Wilson [2] in 1974. For its first five years or so it was a subject studied via analytic calculations. Then in 1979 Creutz, Jacobs, and Rebbi [3] performed the first numerical studies of a lattice gauge theory using Monte Carlo simulation, and over the next few years the field was transformed into one in which numerical methods combined with analytic methods to study nonperturbative behavior. By the late 1980's the field was dominated by very professional large scale simulations of QCD on supercomputers. In the last few years some members of the lattice community have been developing techniques for reducing the size of numerical simulations. These techniques rely heavily on modern work on the renormalization group and effective actions. Some of them actually work: some lattice calculations can now be done on work stations. Some of the techniques may have a wider range of applicability than lattice QCD.

Most of the theoretical ideas that this audience might find interesting are from the pre-computer days of lattice gauge theory. I will begin by describing

how gauge symmetry is realized on the lattice and then show how one studies confinement in the strong coupling limit. Next, I will describe strong-weak coupling duality in the context of lattice models. (This is the only place where I know how to explicitly perform a duality transformation on the field variables.) I will next describe how lattice methods are used to obtain qualitative insight into the behavior of various model systems, without using the computer. Then the subject will change to QCD. I will describe how one performs Monte Carlo simulations, and show the state of the art in lattice calculations of hadron spectroscopy. In one lecture I will talk about the connection between bare actions, effective actions, and scaling, and how this connection is being used to construct "improved actions" for QCD. I will present examples to show the extent to which they actually do improve. Two case studies: glueballs, and the calculation of $\alpha_s(M_Z)$ from the lattice, will conclude the review.

2 Gauge Field Basics

2.1 Beginnings

The lattice is a cutoff which regularizes the ultraviolet divergences of quantum field theories. As with any regulator, it must be removed after renormalization. Contact with experiment only exists in the continuum limit, when the lattice spacing is taken to zero.

We are drawn to lattice methods by our desire to study nonperturbative phenomena. Older regularization schemes are tied closely to perturbative expansions: one calculates a process to some order in a coupling constant; divergences are removed order by order in perturbation theory. The lattice, however, is a nonperturbative cutoff. Before a calculation begins, all wavelengths less than a lattice spacing are removed. Generally one cannot carry out analytical studies of a field theory for physically interesting parameter values. However, lattice techniques lend themselves naturally to implementation on digital computers, and one can perform more-or-less realistic simulations of quantum field theories, revealing their nonperturbative structure, on present day computers. I think it is fair to say that little of the quantitative results about QCD which have been obtained in the last decade, could have been gotten without the use of numerical methods.

On the lattice we sacrifice Lorentz invariance but preserve all internal symmetries, including local gauge invariance. This preservation is important for nonperturbative physics. For example, gauge invariance is a property of the continuum theory which is nonperturbative, so maintaining it as we pass to the lattice means that all of its consequences (including current conservation

and renormalizability) will be preserved.

It is very easy to write down an action for scalar fields regulated by a lattice. One just replaces the space-time coordinate x_μ by a set of integers n_μ ($x_\mu = an_\mu$, where a is the lattice spacing). Field variables $\phi(x)$ are defined on sites $\phi(x_n) \equiv \phi_n$, The action, an integral over the Lagrangian, is replaced by a sum over sites

$$\beta S = \int d^D x \mathcal{L} \to a^4 \sum_n \mathcal{L}(\phi_n). \tag{1}$$

and the generating functional for Euclidean Green's functions is replaced by an ordinary integral over the lattice fields

$$Z = \int (\prod_n d\phi_n) e^{-\beta S}. \tag{2}$$

Gauge fields are a little more complicated. They carry a space-time index μ in addition to an internal symmetry index a ($A^a_\mu(x)$) and are associated with a path in space $x_\mu(s)$: a particle traversing a contour in space picks up a phase factor

$$\psi \to P(\exp\ ig \int_s dx_\mu A_\mu)\psi \tag{3}$$

$$\equiv U(s)\psi(x). \tag{4}$$

P is a path-ordering factor analogous to the time-ordering operator in ordinary quantum mechanics. Under a gauge transformation g, $U(s)$ is rotated at each end:

$$U(s) \to g^{-1}(x_\mu(s))U(s)g(x_\mu(0)). \tag{5}$$

These considerations led Wilson [2] to formulate gauge fields on a space-time lattice, as follows:

The fundamental variables are elements of the gauge group G which live on the links of a D-dimensional lattice, connecting x and $x+\mu$: $U_\mu(x)$, with $U_\mu(x+\mu)^\dagger = U_\mu(x)$

$$U_\mu(n) = \exp(igaT^a A^a_\mu(n)) \tag{6}$$

for $SU(N)$. (g is the coupling, a the lattice spacing, A_μ the vector potential, and T^a is a group generator).

Under a gauge transformation link variables transform as

$$U_\mu(x) \to V(x)U_\mu(x)V(x+\hat{\mu})^\dagger \tag{7}$$

and site variables as

$$\psi(x) \to V(x)\psi(x) \tag{8}$$

so the only gauge invariant operators we can use as order parameters are matter fields connected by oriented "strings" of U's (Fig. 1a)

$$\bar{\psi}(x_1)U_\mu(x)U_\mu(x+\hat{\mu})\dots\psi(x_2) \tag{9}$$

or closed oriented loops of U's (Fig. 1b)

$$\mathrm{Tr}\dots U_\mu(x)U_\mu(x+\hat{\mu})\dots \to \mathrm{Tr}\dots U_\mu(x)V^\dagger(x+\hat{\mu})V(x+\hat{\mu})U_\mu(x+\hat{\mu})\dots. \tag{10}$$

An action is specified by recalling that the classical Yang-Mills action involves the curl of A_μ, $F_{\mu\nu}$. Thus a lattice action ought to involve a product of U_μ's around some closed contour. In fact, there is enormous arbitrariness at this point. We are trying to write down a bare action. So far, the only requirement we want to impose is gauge invariance, and that will be automatically satisfied for actions built of powers of traces of U's around closed loops, with arbitrary coupling constants. If we assume that the gauge fields are smooth, we can expand the link variables in a power series in $gaA'_\mu s$. For almost any closed loop, the leading term in the expansion will be proportional to $F^2_{\mu\nu}$. We might want our action to have the same normalization as the continuum action. This would provide one constraint among the lattice coupling constants.

The simplest contour has a perimeter of four links. In $SU(N)$

$$\beta S = \frac{2N}{g^2}\sum_n\sum_{\mu>\nu}\mathrm{Re\ Tr}\left(1-U_\mu(n)U_\nu(n+\hat{\mu})U^\dagger_\mu(n+\hat{\nu})U^\dagger_\nu(n)\right). \tag{11}$$

This action is called the "plaquette action" or the "Wilson action" after its inventor.

Note Elitzur's theorem: [4] only gauge invariant quantities have nonzero expectation values.

Let us see how this action reduces to the standard continuum action. Specializing to the U(1) gauge group,

$$S = \frac{1}{g^2}\sum_n\sum_{\mu>\nu}\mathrm{Re}\ (1-\exp(iga[A_\mu(n)+A_\nu(n+\hat{\mu})-A_\mu(x+\hat{\nu})-A_\nu(n)])). \tag{12}$$

The naive continuum limit is taken by assuming that the lattice spacing a is small, and Taylor expanding

$$A_\mu(n+\hat{\nu}) = A_\mu(n) + a\partial_\nu A_\mu(n) + \dots \tag{13}$$

so the action becomes

$$S \quad = \tfrac{1}{g^2}\textstyle\sum_n\sum_{\mu>\nu}1-\mathrm{Re}\ (\exp(iga[a(\partial_\nu A_\mu-\partial_\mu A_\nu)+O(a^2)])) \tag{14}$$

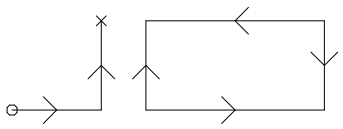

Figure 1: Gauge invariant observables are either (a) ordered chains ("strings") of links connecting quarks and antiquarks or (b) closed loops of link variables.

$$= \tfrac{1}{4g^2} a^4 \sum_n \sum_{\mu\nu} g^2 F_{\mu\nu}^2 + \ldots \tag{15}$$

$$= \tfrac{1}{4} \int d^4x F_{\mu\nu}^2 \tag{16}$$

transforming the sum on sites back to an integral.

The best way people have found to check for quark confinement is to ask the following question: In a world in which there are no light quarks, what is the potential $V(R)$ between a heavy $q\bar{q}$ pair? If the limit as R goes to infinity of $V(R)$ is infinite, we have confinement, if not, quarks are not confined. $V(R)$ can be computed by considering the partition function in Euclidean space for gauge fields in the presence of an external current distribution:

$$Z_J = \int [dU] \exp(-\beta S + i \int J_\mu A_\mu d^4x). \tag{17}$$

(for a non-Abelian gauge group insert color sums $J_\mu^a A_\mu^a$.) If J_μ represents a point particle moving along a world line, it is a δ-function on that world line (parameterized by ℓ_μ):

$$i \int J_\mu A_\mu d^4x = i \oint A_\mu dl_\mu. \tag{18}$$

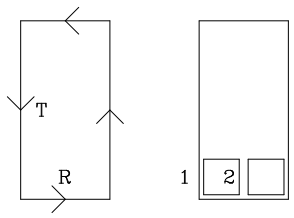

Figure 2: An $R \times T$ Wilson loop (a) and the pattern of tiling which occurs when it is evaluated in strong coupling (b).

Gauge invariance, which implies current conservation, says that the current line cannot end, and so the loop is a closed loop. Let's make it rectangular for simplicity, extending a distance R in some spatial direction and a distance T in the Euclidean time direction. This is the famous Wilson loop. (See Fig. 2a.)

Z_J describes the loop immersed in a sea of gluons. We can think of it as the partition function for a $q\bar{q}$ pair which is created at $t = 0$, pulled apart a distance R, and then allowed to annihilate at a time T later.

To find the pair's energy, differentiate $\ln(Z)$ with respect to T (physically, we are measuring the response of the system as we stretch the loop a bit). [5] But this is not quite right. This calculation will include the vacuum energy of the gluons, which diverges. What we really want is the change in energy of the system when we include the pair and when it is not present:

$$E_{q\bar{q}} = -\frac{\partial}{\partial T}[\ln Z_J - \ln Z_{J=0}] \tag{19}$$

$$= -\frac{\partial}{\partial T} \ln(Z_J/Z_{J=0}) \tag{20}$$

$$= -\frac{\partial}{\partial T} \ln \frac{\int [dU] e^{-\beta S} e^{i \int A \cdot dl}}{\int [dU] e^{-\beta S}} \tag{21}$$

$$= -\frac{\partial}{\partial T} \ln \langle W \rangle_{J=0} \tag{22}$$

where $\langle W \rangle$ is the expectation value of the Wilson loop in the background gluon field. Thus the behavior of $\langle W \rangle$ will tell us whether we have confinement or not.

For example, if $\langle W \rangle \simeq \exp(-m(2R + 2T))$ (a so-called "perimeter law") then $E = 2m$, and m can be interpreted as the quark mass. The energy of the pair is independent of R so that the quarks can separate arbitrarily far apart. However, if $\langle W \rangle \simeq \exp(-\sigma RT)$ (an "area law"), $E = \sigma R$, and quarks are confined with a linear confinement potential. The parameter σ is called the "string tension". In general, $\ln W$ is complicated: $-\ln\langle W \rangle = \sigma RT + 2m(R + T) + \text{constant } + T/R + \ldots$ Nevertheless, any area law term will dominate at large R and T and the theory will confine. Notice that this confinement test will fail in the presence of light dynamical fermions. As we separate the heavy $Q\bar{Q}$ pair, at some point it will become energetically favorable to pop a light $\bar{q}q$ pair out of the vacuum, so that we are separating two color singlet mesons. The Wilson loop will show a perimeter law behavior.

Now let us give an explicit demonstration of confinement for U(1) gauge theory. [6] The Haar measure for $U(1)$ is ($\theta_\mu = gaA_\mu$)

$$\int dU = \int_{-\pi}^{\pi} \frac{d\theta}{2\pi} \tag{23}$$

and

$$Z = \int [dU] \exp(-\beta S) \tag{24}$$

where S is given by Eq. 11.

Strong coupling corresponds to small β. Now we write down two trivial (but useful) results:

$$\int_{-\pi}^{\pi} \frac{d\theta}{2\pi} e^{i(\theta+\phi)} = 0 \tag{25}$$

$$\int_{-\pi}^{\pi} \frac{d\theta}{2\pi} e^{i(\theta+\phi_1)} e^{-i(\theta+\phi_2)} = e^{i(\phi_1-\phi_2)} \tag{26}$$

For small β we may expand the exponential in Z as a power series in β:

$$Z = \int \prod_{links} \frac{d\theta}{2\pi} \prod_{plaquettes} (1 + \beta(\mathrm{Tr}U_p + \text{h. c.} + \ldots) \tag{27}$$

$$= 1 + O(\beta^2) \tag{28}$$

since all linear terms vanish.

Let us compute the expectation value of an L × T Wilson loop (Fig. 2a): There are LT plaquettes enclosed by it.

$$\langle W(L,T)\rangle = \frac{1}{Z}\int \prod \frac{d\theta}{2\pi} \exp(i\sum_{WL}\theta) \prod_{plaquettes} (1+\beta\cos(\sum\theta)+\ldots) \quad (29)$$

It's easy to convince one's self that W is proportional to β^{LT}. Pick one link on the boundary to integrate. We need a term in $\exp(-S)$ to contribute and cancel the phase of the boundary link appearing in the Wilson loop (link 1 of Fig. 2b). Now we simultaneously need another $O(\beta)$ term to cancel the phases of link 2 (of Fig. 2b). Only if we "tile" the whole loop as shown do we get a nonzero expectation value; each plaquette contributes a factor β so

$$\langle W(L,T)\rangle \sim \beta^{LT} \quad (30)$$

$$E_{q\bar{q}} = \sigma L \quad (31)$$

$$\sigma = -\ln\beta \quad (32)$$

This is confinement by linear potential. The calculation can be generalized to all gauge groups. In the strong coupling limit, any lattice gauge theory shows confinement. This calculation was first done by Wilson [2] and was the first demonstration of quark confinement in a field theory in more than two space-time dimensions, albeit in an unphysical limit. This result had a lot to do with the early interest in lattice gauge theory: one has an approximation in which confinement is automatic.

2.2 Taking The Continuum Limit, and Producing a Number in MeV

When we define a theory on a lattice the lattice spacing a is an ultraviolet cutoff and all the coupling constants in the action are the bare couplings defined with respect it. When we take a to zero we must also specify how $g(a)$ behaves. The proper continuum limit comes when we take a to zero holding physical quantities fixed, not when we take a to zero holding the couplings fixed.

On the lattice, if all quark masses are set to zero, the only dimensionful parameter is the lattice spacing, so all masses scale like $1/a$. Said differently, one computes the dimensionless combination $am(a)$. One can determine the lattice spacing by fixing one mass from experiment. Then all other dimensionful quantities can be predicted.

Now imagine computing some masses at several values of the lattice spacing. (Pick several values of the bare parameters at random and calculate masses for each set of couplings.) Our calculated mass ratios will depend on

the lattice cutoff. The typical behavior will look like

$$(am_1(a))/(am_2(a)) = m_1(0)/m_2(0) + O(m_1 a) + O((m_1 a)^2) + \ldots \qquad (33)$$

The leading term does not depend on the value of the UV cutoff, while the other terms do. The goal of a lattice calculation (like the goal of almost any calculation in quantum field theory) is to discover the value of some physical observable as the UV cutoff is taken to be very large, so the physics is in the first term. Everything else is an artifact of the calculation. We say that a calculation "scales" if the $a-$dependent terms in Eq. 33 are zero or small enough that one can extrapolate to $a = 0$, and generically refer to all the $a-$dependent terms as "scale violations."

We can imagine expressing each dimensionless combination $am(a)$ as some function of the bare coupling(s) $\{g(a)\}$, $am = f(\{g(a)\})$. As $a \to 0$ we must tune the set of couplings $\{g(a)\}$ so

$$\lim_{a\to 0} \frac{1}{a} f(\{g(a)\}) \to \text{constant}. \qquad (34)$$

From the point of view of the lattice theory, we must tune $\{g\}$ so that correlation lengths $1/ma$ diverge. This will occur only at the locations of second (or higher) order phase transitions in the lattice theory.

Recall that the β-function is defined by

$$\beta(g) = a\frac{dg(a)}{da} = \frac{dg(a)}{d\ln(1/\Lambda a)}. \qquad (35)$$

(There is actually one equation for each coupling constant in the set. Λ is a dimensional parameter introduced to make the argument of the logarithm dimensionless.) At a critical point $\beta(g_c) = 0$. Thus the continuum limit is the limit

$$\lim_{a\to 0} \{g(a)\} \to \{g_c\}. \qquad (36)$$

Continuum QCD is a theory with one dimensionless coupling constant. In QCD the fixed point is $g_c = 0$ so we must tune the coupling to vanish as a goes to zero.

Pushing this a little further, the two-loop β-function is prescription independent,

$$\beta(g) = -b_1 g^3 + b_2 g^5, \qquad (37)$$

and so if we think that the lattice theory is reproducing the continuum, and if we think that the coupling constant is small enough that the two-loop beta-

function is correct, we might want to observe perturbative scaling, or "asymptotic scaling", m/Λ fixed, or a varying with g as

$$a\Lambda = (\frac{1}{g^2(a)})^{b_2/(2b_1^2)} \exp(-\frac{1}{b_1 g^2(a)}). \tag{38}$$

Please note that asymptotic scaling is not scaling. Scaling means that dimensionless ratios of physical observables do not depend on the cutoff. Asymptotic scaling involves perturbation theory and the definition of coupling constants. One can have one without the other. (In fact, one can always define a coupling constant so that one quantity shows asymptotic scaling.)

And this is not all. There are actually two parts to the problem of producing a number to compare with experiment. One must first see scaling. Then one needs to set the scale by taking some experimental number as input. A complication that you may not have thought of is that the theory we simulate on the computer is different from the real world. For example, a commonly used approximation is called the "quenched approximation": one neglects virtual quark loops, but includes valence quarks in the calculation. The pion propagator is the propagator of a $\bar{q}q$ pair, appropriately coupled, moving in a background of gluons. This theory almost certainly does not have the same spectrum as QCD with six flavors of dynamical quarks with their appropriate masses. (In fact, an open question in the lattice community is, what is the accuracy of quenched approximation.) Using one mass to set the scale from one of these approximations to the real world might not give a prediction for another mass which agrees with experiment. We will see examples where this is important.

3 Abelian Duality with a Lattice Regulator

"Every theorist knows" that a phase with electrical confinement (area law for Wilson loops, etc.) is has a dual description in terms of magnetic variables which are screened, in analogy with the Meissner effect in a superconductor. There are many sources for this intuition. The one that people in my generation point to are lattice calculations in Abelian gauge and spin models. In these models one can explicitly perform the duality transformation. In some models (notably the $d = 2$ U(1) spin model and the $d = 3$ gauge model) one can solve the dynamics sufficiently well to understand the role of magnetic variables: the Kosterlitz-Thouless vortex-unbinding transition in the former case, and Polyakov's demonstration of confinement in the latter. Classic references include [7] [8] [9] [10].

Let's begin with a $d = 2$ $U(1)$ (or $O(2)$) spin model. On each site of the lattice there is a unit-length spin $\vec{s}(x)$, which can be labeled by an angle (the orientation of the spin) $\phi(x)$. We assume nearest neighbor spins interact via $\mathcal{H} = \sum_x (1 - \vec{s}(i) \cdot \vec{s}(i + \hat{\mu})) = \sum_{x,\mu} (1 - \cos(\phi(x) - \phi(x + \hat{\mu})))$. The partition function is

$$Z = \int_{\pi}^{\pi} [d\phi(x)] \exp(-\beta \mathcal{H}). \tag{39}$$

Let's perform the Fourier transform

$$\exp\big(-\beta(1 - \cos(\theta))\big) = \sum_{-\infty}^{\infty} e^{in\theta} f_n(\beta) \tag{40}$$

with

$$f_n(\beta) \simeq \frac{1}{\sqrt{2\pi\beta}} e^{-n^2/(2\beta)} \tag{41}$$

to rewrite the partition function as

$$Z = \int [d\phi] \prod_{x,\mu} \sum_{n_\mu(x)=-\infty}^{\infty} e^{i \sum n_\mu(x)(\phi(x+\hat{\mu}) - \phi(x))} e^{-\sum_{x,\mu} n_\mu(x)^2/(2\beta)}. \tag{42}$$

We can now integrate over the spin variables, which constrains the $n'_\mu s$:

$$\int d\phi(x) e^{i\phi(x)[n_\mu(x-\mu) - n_\mu(x)]} = \delta_{\nabla_\mu n_\mu, 0}. \tag{43}$$

We can solve the constraint by introducing

$$n_\mu(x) = \epsilon_{\mu\nu} \nabla_\nu n(x) \tag{44}$$

which gives a partition function

$$Z = \prod_x \sum_{n(x)=-\infty}^{\infty} \exp(-\sum_{r,\mu} \frac{(\nabla_\mu n)^2}{2\beta}), \tag{45}$$

but at large β the sums converge slowly. The Poisson resummation formula

$$\sum_l \delta(x - l) = \sum_m e^{2\pi i m x} \tag{46}$$

or

$$\sum_l g(l) = \sum_m \int d\phi g(\phi) e^{2\pi i m \phi} \tag{47}$$

allows us to rewrite the partition function as

$$Z = \prod_x \int [d\phi(x)] \sum_{m(x)=-\infty}^{\infty} \exp\big(- \sum_{r,\mu} (\frac{\nabla_\mu \phi)^2}{2\beta}) \exp(2\pi i \sum_r m(r)\phi(r)\big) \quad (48)$$

or

$$Z = Z_{m=0} Z_{m\neq 0} \quad (49)$$

where

$$Z_{m=0} = \int [d\phi(x)] \exp(-\sum_{r,\mu} \frac{(\nabla_\mu \phi)^2}{2\beta}) \quad (50)$$

is a free massless field theory (these are "spin waves" in condensed-matter jargon), and the second term is a "vortex component,"

$$Z_{m\neq 0} = \prod_x \sum_{m(x)=-\infty}^{\infty} \exp\big(- 2\pi^2 \beta m(x) G(x-x') m(x')\big) \quad (51)$$

where

$$\nabla^2 G = \delta(x-x'). \quad (52)$$

That is, we have rewritten the original partition function in terms of a set of variables which live on the sites, take on integer values (0, ± 1, $\pm 2, \ldots$), and interact by long-range Coulomb interactions. These variables are called (depending on your dialect) vortices, defects, solitons, monopoles, or instantons. Clearly, the $\beta \to \infty$ phase has few vortices, and the low β phase will have many. This model has a phase transition at intermediate β mediated by the condensation of vortices [7].

The algebra is similar in other dimensions. For $d = 3$ the constraint is

$$\nabla_\mu n_\mu = 0 \to n_\mu = \epsilon_{\mu\nu\lambda} \nabla_\nu n_\lambda(x) \quad (53)$$

and if we impose a further "gauge constraint"

$$\nabla_\lambda n_\lambda = 0 \quad (54)$$

we arrive at the partition function for a system of interacting, conserved, oriented "vortex strings"

$$Z(string) = \prod_{x,\mu} \sum_{m_\mu(x)=-\infty}^{\infty} \exp\big(-2\pi^2 \beta \sum_{x,x',\mu,\nu} m_\mu(x) G_{\mu,\nu}(x-x') m_\nu(x')\big)|_{\nabla_\mu m_\mu = 0}. \quad (55)$$

Again,

$$\nabla^2 G_{\mu\nu} = \delta_{\mu\nu}\delta(x) \tag{56}$$

and the oriented strings have a Coulomb interaction.

U(1) gauge theories with the Wilson action

$$\cos(\theta_{\mu\nu}(x)) = \cos(\theta_\mu(x) + \theta_\nu(x+\mu) - \theta_\mu(x+\nu) - \theta_\nu(x)) \tag{57}$$

can be treated similarly. The Fourier transform introduces a constraint

$$\exp(il_{\mu\nu}\theta_{\mu\nu}) \to \delta_{\nabla_\mu l_{\mu\nu},0}. \tag{58}$$

In three dimensions the constraint is solved by setting $l_{\mu\nu} = \epsilon_{\mu\nu\lambda}\partial_\lambda l$. We have a system of interacting (charged) point defects: monopoles or instantons. In four dimensions the constraint is solved by setting $l_{\mu\nu} = \epsilon_{\mu\nu\lambda}\partial_\lambda l_\sigma$ with $\partial_\sigma l_\sigma = 0$. This is a system of interacting monopole world lines. For more details about "what comes next," see [9] [10] [11].

3.1 Polyakov's Solution of 3-d U(1) Gauge Theory

Polyakov showed that the $d = 3$ U(1) gauge theory is permanently confining for all values of the gauge coupling. The calculation begins by considering the grand partition function for a gas of monopoles, where we restrict the possible charges to ± 1. (In keeping with the spirit of the original demonstrations, all my numerical factors are probably wrong.) The monopole fugacity $\zeta = \exp(-1/e^2)$. The partition function is

$$Z = \sum_N \sum_{q_J=\pm 1} \frac{\zeta^N}{N!} \int dx_1 \dots dx_N \exp(-\beta\pi^2 \sum_{a\neq b} \frac{q_a q_b}{|x_a - x_b|}) \tag{59}$$

or

$$Z = \int [d\chi] \exp(-\frac{\pi}{\beta}\int dx (\nabla\chi)^2) \sum_N \sum_{q=\pm 1} \frac{\zeta^N}{N!} dx_1 \dots dx_N e^{i\sum_j q(x_j)\chi(x_j)}. \tag{60}$$

We can sum over the charges on a site $\sum_q \to \int dx (e^{i\chi} + e^{-i\chi})$ and exponentiate to produce a sine-Gordon Lagrangian

$$Z = \int [d\chi] \exp(-\frac{\pi}{\beta}\int dx [(\nabla\chi)^2 - M^2 \cos\chi]) \tag{61}$$

where $M^2 = \beta\zeta/\pi$. Now let's introduce a Wilson loop into the calculation. We reverse the derivation of the Wilson loop of the last lecture to write

$$\begin{aligned} W(C) = & \quad \exp i \oint_C A \cdot dl & (62) \\ = & \quad \exp i \int d^4x J_{ext} \cdot A & (63) \\ = & \quad \exp i \sum_r q(r)\eta(r) & (64) \end{aligned}$$

where η is the magnetic scalar potential arising from the external current loop, $\nabla^2\eta = \vec{\nabla} \cdot \vec{B}_{ext} = \rho$. We repeat the derivation including the external scalar potential and find

$$Z(\eta) = \int [d\chi] \exp(-\frac{\pi}{\beta} \int dx[(\nabla(\chi - \eta))^2 - M^2 \cos\chi]). \tag{65}$$

We solve the integral by steepest descent, and find

$$Z(\eta) = \exp\big(-\frac{\pi}{\beta} \int dx[(\nabla(\chi_{cl} - \eta))^2 - M^2 \cos\chi_{cl}]\big) \tag{66}$$

where

$$\nabla^2\chi_{cl} = M^2 \sin\chi_{cl} + \nabla^2\eta \tag{67}$$

What is the solution? $\chi \neq 0$ only near the sheet and $\chi \simeq \exp(-M|z|)$ moving transversely away from the sheet, so $Z(\eta) \simeq \exp(-\gamma \times area)$ where $\gamma \simeq \pi/\beta \times M^2 \times 1/M \simeq \exp(-1/e^2)$. This is the signal of linear confinement. Hence the intuition: electrical confinement is due to the free monopoles which screen external magnetic fields.

4 Simple Lattice Intuition

Let's finally consider some variations on these models. Z_N models are like $U(1)$ models, except the variables are restricted to $\theta = 2\pi j/N$, $j = 1 \ldots N$. They can have three phases: a low-beta phase with many defects, a high-beta magnetically-ordered or "Higgs" phase, and possibly a spin wave phase at intermediate coupling. The generic phase diagram is shown in Fig. 3. It is easy to estimate the location of the magnetic ordering transition: Fluctuations in θ go like $(\delta\theta)^2 \simeq \langle\theta^2\rangle \simeq 1/\beta$, but if this $\delta\theta < 1/N$ the spin cannot fluctuate from one allowed value to another one, and the system freezes. This happens at $\beta_c \simeq N^2$.

While the spin-wave phase is "just free field theory," in two dimensions the free behavior of the angular variable is

$$\langle\phi_i\phi_j\rangle \simeq \frac{1}{\beta}\log(\frac{r_{ij}}{r_0}). \tag{68}$$

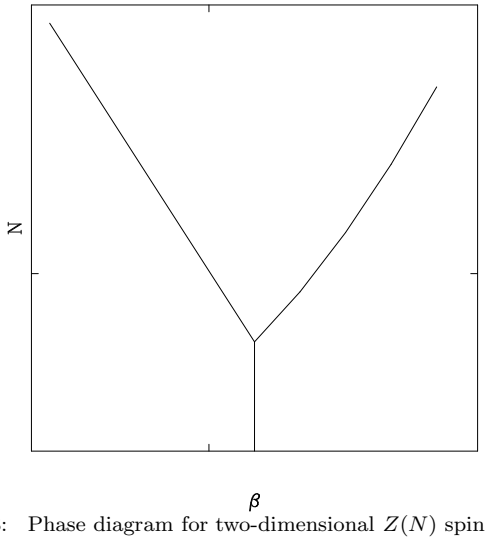

Figure 3: Phase diagram for two-dimensional $Z(N)$ spin models.

However, the spin-spin correlator is

$$\langle s_i \cdot s_j \rangle = \quad \langle e^{i(\phi_i - \phi_j)} \rangle \tag{69}$$

$$= |r_{ij}|^{(1/\beta)} \tag{70}$$

whose exponent varies continuously with the coupling. The continuous variation in a critical index with an input parameter signals that the system is always critical and one speaks of the system as being characterized by a "line of critical points."

We already saw that U(1) gauge models with a lattice regulator confine in three Euclidean dimensions. All lattice gauge theories confine in two Euclidean dimensions. The demonstration is straightforward. Write down the partition function and gauge fix so that all the links in one direction (direction 2, in the following) are set to the identity. (It may be necessary to take open boundary conditions to do this.) The partition function becomes

$$Z = \int \prod dU_1(x) \exp(\beta Tr U_1(x) U_1^\dagger(x + \hat{2})). \tag{71}$$

Now perform a second set of gauge transformations $U_1(x) = U_1(x)U_1^\dagger(x + \hat{2})$, etc. The partition function factorizes into a produce of one-plaquette actions

$$Z = [\int dU \exp(\beta Tr U)]^{L \cdot T}. \tag{72}$$

The partition function has no singularities unless the single link integral does (this can happen at large-N, for example). It is easy to repeat the calculation for the Wilson loop and find an area law.

Monte Carlo simulations show that four-dimensional U(1) gauge theory has a confining phase at strong coupling, apparently induced by monopole condensation as in three dimensions, and a phase transition at $e^2 \simeq 1$ into a weak-coupling Coulomb phase. In that phase the relic monopole loops slightly renormalize the electric charge. The order of the transition was controversial for many years, but recent studies favor second order [12]. If it were first order, the theory would have a continuum limit only in the Coulomb phase. If the transition is second order, one could define a continuum confined U(1) theory by approaching the phase transition from within the confined phase.

Z(N) gauge theories in four dimensions have a phase diagram similar to spin models. There is a strong-coupling confinement phase, a magnetically-ordered Higgs phase at large β, and at larger N, an intermediate coupling Coulomb phase. When there are only two phases, the deconfinement transition is first order.

There are many cases where the lattice can be used to provide insight into a physical system, without the need for simulation. An example of such a situation is the gauge-Higgs system, with a (schematic) Lagrange density

$$\mathcal{L} = \mathcal{L}_{gauge} + (D_\mu \Phi)^2 - V(\Phi). \tag{73}$$

It is often useful to convert to radial and angular variables: $\Phi = \rho\phi$ with $|\phi|^2 = 1$. Then if we take $V(\Phi) = \lambda(\Phi^2 - f^2)^2 = \lambda(\rho^2 - f^2)^2$, we can freeze out the radial mode by taking the $\lambda \to \infty$ limit, so $\langle\rho\rangle = f$. Replacing the gradient by a lattice difference, one can then write the action in terms of two coupling constants as

$$\mathcal{L} = \beta_g Tr(1 - UUUU) - \beta_h \phi_x^\dagger U_\mu(x)\phi(x+\mu). \tag{74}$$

The two coupling constants describe a plane of possible theories. One studies the continuum behavior of these theories on the lattice by finding all the critical points/lines in the phase diagram. One recovers continuum physics by tuning couplings to approach those critical points.

One can usually figure out the behavior of the theory on the boundaries of the coupling constant plane without using Monte Carlo, and use Monte Carlo only to explore the interior of the phase diagram. This was a very common game in the days before the lattice community became "professional." Let's see how it works for a gauge-Higgs model.

The first limiting case is $\beta_h = 0$. This is a pure gauge theory, which one has to analyze on its own.

Now $\beta_g = 0$. This is a trivial limit, the strong-coupling confined phase limit. One can see this in two ways. The first way is to realize that there is no gauge interaction, so all the link variables decouple and $\mathcal{L} = \phi^\dagger U \phi$ describes a set of random interactions. All $\langle \phi_i \phi_j \rangle$ correlators vanish away from zero separation. Another way to see this limit is to gauge fix to "unitary gauge" by rotating all the ϕ's to some constant value ϕ_0. Now

$$Z = \int \prod_{x,\mu} dU_\mu(x) \exp(\beta_h \sum_{x,\mu} \phi_0^\dagger U_\mu(x) \phi_0) \tag{75}$$

and again the partition function factorizes in to a product of one-link integrals.

At $\beta_g = \infty$ we gauge-fix to an axial gauge by rotating all the U's to the identity. (Only $U = 1$ configurations are important in the functional integral in this limit.) Now $-\mathcal{L} = \beta_h \phi^\dagger(x) \phi(x + \mu)$ which is a pure spin model. Again, one must analyze it on its own.

Finally, we have $\beta_h \to \infty$. Use unitary gauge again. In this limit $\phi_0^\dagger U_\mu(x) \phi_0$ is forced to its maximum value. If it happens the ϕ transforms under a faithful representation of the gauge group G, only $U = 1$ is allowed. If the representation of ϕ is not faithful, then there is a subgroup H of G in which $U = 1$. Along this line, we then have a gauge theory with gauge group $H \in G$. In the first case the Higgs and confinement phases are likely to be connected [13] (as shown in Fig. 4a). In the second case, the gauge symmetry on the top line is typically a discrete symmetry, there is typically a first order phase transition (which extends into the phase diagram) and one must resort to Monte Carlo to see if the phases are connected or separated. Schematic phase diagrams for Z_2 gauge-Z_2 spin and Z_6 gauge-Z_3 spin models [14] are shown in Figs. 4a and b.

Finally, a few words about fermions (see the next section for details). It is easy to study vectorlike theories on the lattice, and easiest to study multiples of 2 or 4 degenerate flavors of fermions. It is reasonably easy to study the chiral properties of model theories, although taking the chiral limit in a computer simulation is hard. Common games to play are to measure $\langle \bar{\psi} \psi \rangle$ in a simulation at finite fermion mass and to extrapolate to zero mass. With Kogut-Susskind fermions, this operator is only multiplicatively renormalized, and so one can see if it vanishes at zero quark mass or extrapolates to some finite limit. One can also compute the pion mass and ask whether $m_\pi^2 \simeq m_q$. Only fermion actions which are bilinear, $S = \bar{\psi} M \psi$ for any matrix M, can be simulated on the computer, but if one has a four-fermion interaction, the Hubbard-Stratonovich transformation

$$\exp -(\bar{\psi}\psi)^2 = \int d\phi \exp -(\bar{\psi}\psi\phi + \phi^2) \tag{76}$$

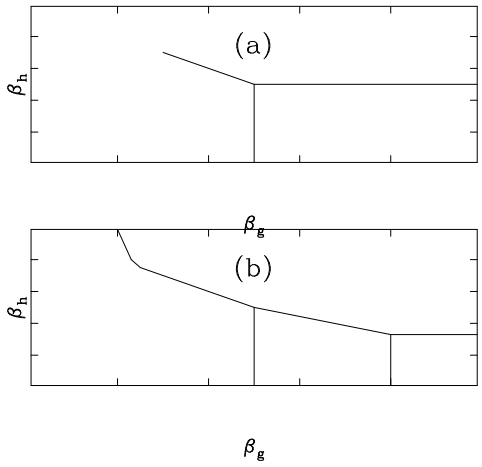

Figure 4: Phase diagrams for (a) Z_2 gauge-Z_2 spin and and (b) Z_6 gauge-Z_3 spin models.

allows four-fermion interaction models to be converted into Yukawa models (said differently, four-fermion interaction models are equivalent to Yukawa models [15]), which the computer (and maybe the physicist) knows how to solve.

5 Standard Methods for Spectroscopy

5.1 Relativistic Fermions on the Lattice

Defining fermions on the lattice presents a new problem: doubling. The naive procedure of discretizing the continuum fermion action results in a lattice model with many more low energy modes than one originally anticipated. Let's illustrate this with free field theory.

The free Euclidean fermion action in the continuum (in four dimensions) is

$$S = \int d^4x [\bar{\psi}(x)\gamma_\mu \partial_\mu \psi(x) + m\bar{\psi}(x)\psi(x)]. \tag{77}$$

One obtains the so-called naive lattice formulation by replacing the derivatives by symmetric differences: we explicitly introduce the lattice spacing a in the denominator and write

$$S_L^{naive} = \sum_{n,\mu} \bar{\psi}_n \frac{\gamma_\mu}{2a}(\psi_{n+\mu} - \psi_{n-\mu}) + m \sum_n \bar{\psi}_n \psi_n. \tag{78}$$

The propagator is:

$$G(p) = (i\gamma_\mu \sin p_\mu a + ma)^{-1} = \frac{-i\gamma_\mu \sin p_\mu a + ma}{\sum_\mu \sin^2 p_\mu a + m^2 a^2} \tag{79}$$

We identify the physical spectrum through the poles in the propagator, at $p_0 = iE$:

$$\sinh^2 Ea = \sum_j \sin^2 p_j a + m^2 a^2 \tag{80}$$

The lowest energy solutions are the expected ones at $p = (0,0,0)$, $E \simeq \pm m$, but there are other degenerate ones, at $p = (\pi,0,0)$, $(0,\pi,0,)$, $\ldots(\pi,\pi,\pi)$. This is a model for sixteen light fermions, not one.

(a) Wilson Fermions

There are two ways to deal with the doublers. The first way is to alter the dispersion relation so that it has only one low energy solution. The other solutions are forced to $E \simeq 1/a$ and become very heavy as a is taken to zero. The simplest version of this solution (and almost the only one seen in the literature until recently) is due to Wilson: add a second-derivative-like term

$$S^W = -\frac{r}{2a} \sum_{n,\mu} \bar{\psi}_n (\psi_{n+\mu} - 2\psi_n + \psi_{n-\mu}) \tag{81}$$

to S^{naive}. The parameter r must lie between 0 and 1; $r = 1$ is almost always used and "$r = 1$" is implied when one speaks of using "Wilson fermions." The propagator is

$$G(p) = \frac{-i\gamma_\mu \sin p_\mu a + ma - r\sum_\mu (\cos p_\mu a - 1)}{\sum_\mu \sin^2 p_\mu a + (ma - r\sum_\mu (\cos p_\mu a - 1))^2}. \tag{82}$$

It has one pair of poles at $p_\mu \simeq (\pm im, 0, 0, 0)$, plus other poles at $p \simeq r/a$. In the continuum these states become infinitely massive and decouple (although decoupling is not trivial to prove).

With Wilson fermions it is conventional not to use not the mass but the "hopping parameter" $\kappa = \frac{1}{2}(ma + 4r)^{-1}$, and to rescale the fields $\psi \to \sqrt{2\kappa}\psi$. The action for an interacting theory is conventionally written

$$S = \sum_n \bar{\psi}_n \psi_n - \kappa \sum_{n\mu} (\bar{\psi}_n (r - \gamma_\mu) U_\mu(n) \psi_{n+\mu} + \bar{\psi}_n (r + \gamma_\mu) U_\mu^\dagger \psi_{n-\mu}). \tag{83}$$

Wilson fermions are closest to the continuum formulation– there is a four component spinor on every lattice site for every color and/or flavor of quark. Constructing currents and states is just like in the continuum.

However, the Wilson term explicitly breaks chiral symmetry. This has the consequence that the zero bare quark mass limit is not respected by interactions; the quark mass is additively renormalized. The value of κ_c, the value of the (bare) hopping parameter at which the pion mass vanishes, is not known a priori before beginning a simulation; it must be computed. This is done in a simulation involving Wilson fermions by varying κ and watching the pion mass extrapolate quadratically to zero as $m_\pi^2 \simeq \kappa_c - \kappa$ ($\kappa_c - \kappa$ is proportional to the quark mass for small m_q).

(b) Staggered or Kogut-Susskind Fermions

In this formulation one reduces the number of fermion flavors by using one component "staggered" fermion fields rather than four component Dirac spinors. The Dirac spinors are constructed by combining staggered fields on different lattice sites.

Let us call the staggered field on site n χ_n and define the matrix field

$$\psi_{\alpha k}(n) = \sum_b (\gamma^{n+b})_{\alpha k} \chi_{n+b} \tag{84}$$

where

$$\gamma^{n+b} = \gamma_1^{n_1+b_1} \gamma_2^{n_2+b_2} \gamma_3^{n_3+b_3} \gamma_4^{n_4+b_4} \tag{85}$$

and b runs over the sites of a hypercube $b = (0,0,0,0)$, (1,0,0,0), ... (1,1,1,1). $\bar{\psi}_{\alpha k}$ is defined analogously,

$$\bar{\psi}_{\alpha k}(n) = \sum_b (\gamma^{n+b})^\dagger_{\alpha k} \bar{\chi}_{n+b}. \tag{86}$$

One interprets the α indices as spin (= 1 to 4) and k as flavor (= 1 to 4). The free action (with $m_q = 0$) is

$$S = \frac{1}{128} \sum \bar{\psi}_n \gamma_\mu (\psi_{n+\mu} - \psi_{n-\mu}) \tag{87}$$

$$= \frac{1}{2} \sum \bar{\chi}_n \eta_{n,\mu} (\chi_{n-\mu} - \chi_{n+\mu}) \tag{88}$$

where $\eta_{n,\mu} = (-1)^{n_1+n_2+n_3+n_4}$. Gauge fields can be added in the standard way, and explicit mass terms give an extra $m_q \sum \bar{\chi}\chi$ term.

Staggered fermions preserve an explicit chiral symmetry as $m_q \to 0$ even for finite lattice spacing, as long as all four flavors are degenerate. They are preferred over Wilson fermions in situations in which the chiral properties of the fermions dominate the dynamics–for example, in studying the chiral restoration/deconfinement transition at high temperature. They also present

a computationally less intense situation from the point of view of numerics than Wilson fermions, for the trivial reason that there are less variables. However, flavor symmetry and translational symmetry are all mixed together. Construction of meson and baryon states (especially the Δ) is more complicated than for Wilson fermions [16].

5.2 Enter the Computer

A "generic" Monte Carlo simulation in QCD breaks up naturally into two parts. In the "configuration generation" phase one constructs an ensemble of states with the appropriate Boltzmann weighting: we compute observables simply by averaging N measurements using the field variables $\phi^{(i)}$ appropriate to the sample

$$\langle \Gamma \rangle \simeq \bar{\Gamma} \equiv \frac{1}{N} \sum_{i=1}^{N} \Gamma[\phi^{(i)}]. \tag{89}$$

As the number of measurements N becomes large the quantity $\bar{\Gamma}$ will become a Gaussian distribution about a mean value. Its standard deviation is roughly [17]

$$\sigma_\Gamma^2 = \frac{1}{N}(\frac{1}{N} \sum_{i=1}^{N} |\Gamma[\phi^{(i)}]|^2 - \bar{\Gamma}^2). \tag{90}$$

The idea of essentially all simulation algorithms is that one constructs a new configuration of field variables from an old one. One begins with some simple field configuration and monitor observables while the algorithm steps along. After some number of steps, the value of observables will appear to become independent of the starting configuration. At that point the system is said to be "in equilibrium" and Eq. 89 can be used to make measurements.

The simplest method for generating configurations is called the Metropolis [18] algorithm. It works as follows: From the old configuration $\{\phi\}$ with action βS, transform the variables (in some reversible way) to a new trial configuration $\{\phi\}'$ and compute the new action $\beta S'$. Then, if $S' < S$ make the change and update all the variables; if not, make the change with probability $\exp(-\beta(S' - S))$.

Why does it work? In equilibrium, the rate at which configurations i turn into configurations j is the same as the rate for the back reaction $j \to i$. The rate of change is (number of configurations) $\times$ (probability of change). Assume for the sake of the argument that $S_i < S_j$. Then the rate $i \to j$ is $N_i P(i \to j)$ with $P(i \to j) = \exp(-\beta(S_j - S_i)$ and the rate $j \to i$ is $N_j P(j \to i)$ with $P(j \to i) = 1$. Thus $N_i/N_j = \exp(-\beta(S_i - S_j))$.

If you have any interest at all in the techniques I am describing, you should write a little Monte Carlo program simulating the two-dimensional Ising model. Incidentally, the favorite modern method for pure gauge models is overrelaxation [19].

One complication for QCD which spin models don't have is fermions. The fermion path integral is not a number and a computer can't simulate fermions directly. However, one can formally integrate out the fermion fields. For n_f degenerate flavors of staggered fermions

$$Z = \int [dU][d\psi][d\bar{\psi}] \exp(-\beta S(U) - \sum_{i=1}^{n_f} \bar{\psi} M \psi) \tag{91}$$

$$= \int [dU] (\det M)^{n_f/2} \exp(-\beta S(U)). \tag{92}$$

(One can make the determinant positive-definite by writing it as $\det(M^\dagger M)^{n_f/4}$.) The determinant introduces a nonlocal interaction among the U's:

$$Z = \int [dU] \exp(-\beta S(U) - \frac{n_f}{4} \mathrm{Tr} \ln(M^\dagger M)). \tag{93}$$

All large scale dynamical fermion simulations today generate configurations using some variation of the microcanonical ensemble. That is, they introduce momentum variables P conjugate to the U's and integrate Hamilton's equations through a simulation time t

$$\dot{U} = iPU \tag{94}$$

$$\dot{P} = -\frac{\partial S_{eff}}{\partial U}. \tag{95}$$

The integration is done numerically by introducing a timestep Δt. The momenta are repeatedly refreshed by bringing them in contact with a heat bath and the method is thus called Refreshed or Hybrid Molecular Dynamics [20].

For special values of n_f (multiples of 2 for Wilson fermions or of 4 for staggered fermions) the equations of motion can be derived from a local Hamiltonian and in that case Δt systematics in the integration can be removed by an extra Metropolis accept/reject step. This method is called Hybrid Monte Carlo [21].

The reason for the use of these small timestep algorithms is that for any change in any of the U's, $(M^\dagger M)^{-1}$ must be recomputed. When Eqn. 95 is integrated all of the U's in the lattice are updated simultaneously, and only one matrix inversion is needed per change of all the bosonic variables.

The major computational problem dynamical fermion simulations face is inverting the fermion matrix M. It has eigenvalues with a very large range– from 2π down to $m_q a$– and in the physically interesting limit of small m_q the matrix becomes ill-conditioned. At present it is necessary to compute at unphysically heavy values of the quark mass and to extrapolate to $m_q = 0$. The standard inversion technique today is one of the variants of the conjugate gradient algorithm [22].

5.3 Spectroscopy Calculations

"In a valley something like a race took place. A little crowd watched bunches of cars, each consisting of two 'ups' and a 'down' one, starting in regular intervals and disappearing in about the same direction. 'It is the measurement of the proton mass,' commented Mr. Strange, 'they have done it for ages. A very dull job, I am glad I am not in the game.' " [23]

Masses are computed in lattice simulations from the asymptotic behavior of Euclidean-time correlation functions. A typical (diagonal) correlator can be written as

$$C(t) = \langle 0|O(t)O(0)|0\rangle. \tag{96}$$

Making the replacement

$$O(t) = e^{Ht} O e^{-Ht} \tag{97}$$

and inserting a complete set of energy eigenstates, Eq. (3.1) becomes

$$C(t) = \sum_n |\langle 0|O|n\rangle|^2 e^{-E_n t}. \tag{98}$$

At large separation the correlation function is approximately

$$C(t) \simeq |\langle 0|O|1\rangle|^2 e^{-E_1 t} \tag{99}$$

where E_1 is the energy of the lightest state which the operator O can create from the vacuum. If the operator does not couple to the vacuum, then in the limit of large t one hopes to to find the mass E_1 by measuring the leading exponential falloff of the correlation function, and most lattice simulations begin with that measurement. If the operator O has poor overlap with the lightest state, a reliable value for the mass can be extracted only at a large time t. In some cases that state is the vacuum itself, in which $E_1 = 0$. Then one looks for the next higher state–a signal which disappears into the constant background. This makes the actual calculation of the energy more difficult.

This is the basic way hadronic masses are found in lattice gauge theory. The many calculations differ in important specific details of choosing the operators $O(t)$.

5.4 Recent Results

Today's supercomputer QCD simulations range from $16^3 \times 32$ to $32^3 \times 100$ points and run from hundreds (quenched) to thousands (full QCD) of hours on the fastest supercomputers in the world.

Results are presented in four common ways. Often one sees a plot of some bare parameter vs. another bare parameter. This is not very useful if one wants to see continuum physics, but it is how we always begin. Next, one can plot a dimensionless ratio as a function of the lattice spacing. These plots represent quantities like Eqn. 33. Both axes can show mass ratios. Examples of such plots are the so-called Edinburgh plot (m_N/m_ρ vs. m_π/m_ρ) and the Rome plot (m_N/m_ρ vs. $(m_\pi/m_\rho)^2$). These plots can answer continuum questions (how does the nucleon mass change if the quark mass is changed?) or can be used to show (or hide) scaling violations. Plots of one quantity in MeV vs. another quantity in MeV are typically rather heavily processed after the data comes off the computer.

Let's look at some examples of spectroscopy, done in the "standard way," with the plaquette gauge action and Wilson or staggered quarks. I will restrict the discussion to quenched simulations because only there are the statistical errors small enough to be interesting to a non-lattice audience. Most dynamical fermion simulations are unfortunately like Dr. Johnson's dog.

Fig. 5 shows a plot of the rho mass as a function of the size of the simulation, for several values of the quark mass (or m_π/m_ρ ratio in the simulation) and lattice spacing ($\beta = 6.0$ is $a \simeq 0.1$ fm and $\beta = 5.7$ is about twice that) [24]. This picture shows that if the box has a diameter bigger than about 2 fm, the rho mass is little affected, but if the box is made smaller, the rho is "squeezed" and its mass rises.

Next we look at an Edinburgh plot, Fig. 6 [24]. The different plotting symbols correspond to different bare couplings or (equivalently) different lattice spacings. This plot shows large scaling violations: mass ratios from different lattice spacings do not lie on top of each other. We can expose the level of scaling violations by taking "sections" through the plot and plot m_N/m_ρ at fixed values of the quark mass (fixed m_π/m_ρ), vs. lattice spacing, in Fig. 7.

Now for some examples of scaling tests in the chiral limit. (Extrapolating to the chiral limit is a whole can of worms on its own, but for now let's assume we can do it.) Fig. 8 shows the nucleon to rho mass ratio (at chiral limit) vs. lattice spacing (in units of $1/m_\rho$) for staggered [24] and Wilson [25] fermions. The "analytic" result is from strong coupling. The two curves are quadratic extrapolations to zero lattice spacing using different sets of points from the staggered data set. The burst is from a linear extrapolation to the Wilson

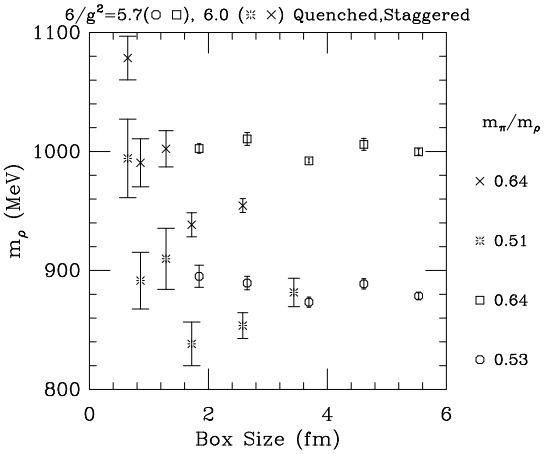

Figure 5: Rho mass vs. box size.

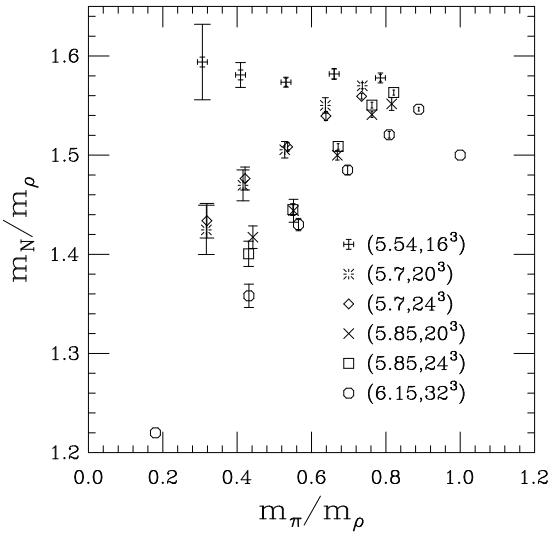

Figure 6: An Edinburgh plot for staggered fermions, from the MILC collaboration.

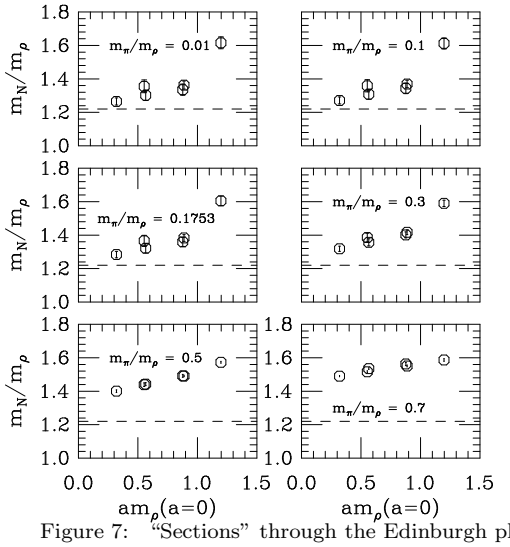

Figure 7: "Sections" through the Edinburgh plot.

data. The reason I show this figure is that one would like to know if the continuum limit of quenched spectroscopy "predicts" the real-world N/ρ mass ratio of 1.22 or not. The answer (unfortunately) depends on how the reader chooses to extrapolate.

Another test [26] is the ratio of the rho mass to the square root of the string tension, Fig. 9. Here the diamonds are staggered data and the crosses from the Wilson action. Scaling violations are large but the eye extrapolates to something close to data (the burst).

Finally, despite Mr. Strange, very few authors have attempted to extrapolate to infinite volume, zero lattice spacing, and to physical quark masses, including the strange quark. One group which did, Butler et al. [25], produced Fig. 10. The squares are lattice data, the octagons are the real world. They look quite similar within errors. Unfortunately, to produce this picture, they had to build their own computer.

6 Bare Actions, Scaling, and Improved Actions

(Disclaimer: It happens that at present there are a number of approaches to "improvement." At present, the words which are used to describe them differ greatly among the different groups, and the physics motivations are quite different. For example, in one approach, ideas based on perturbation theory are

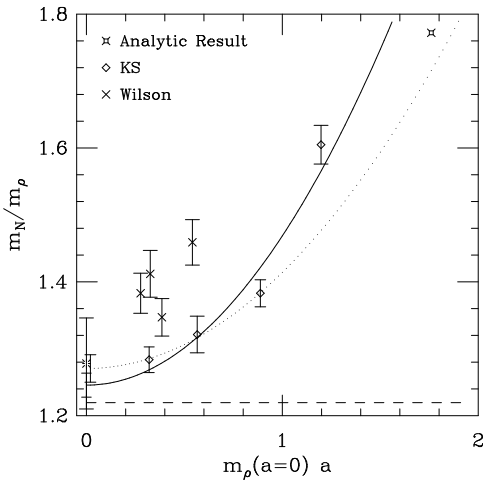

Figure 8: Nucleon to rho mass ratio (at chiral limit) vs. lattice spacing (in units of $1/m_\rho$).

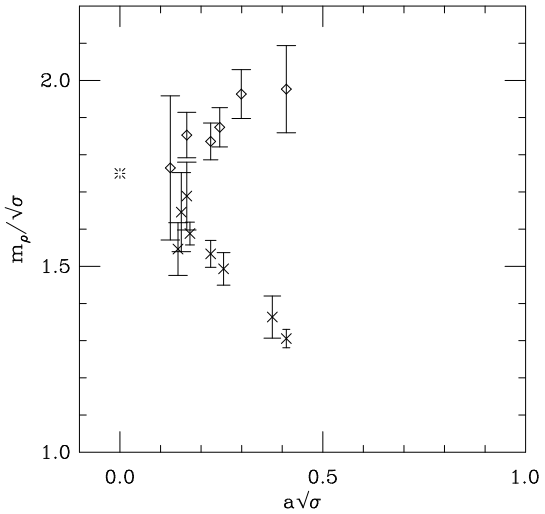

Figure 9: Scaling test for the rho mass in terms of the string tension, with data points labeled as in Fig. 8.

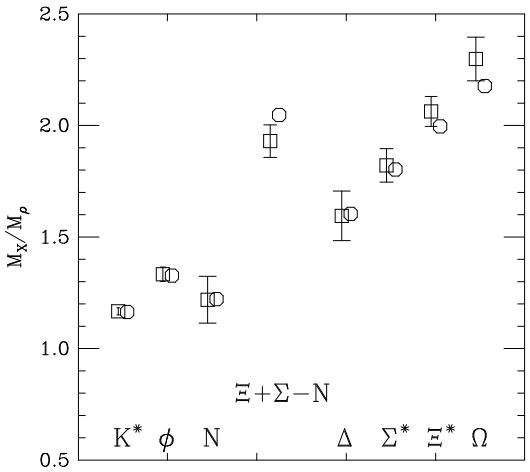

Figure 10: Quenched approximation mass ratios from Ref. 25.

regarded as absolutely crucial while in another approach perturbation theory is said to be completely irrelevant. The particular problems whose solution would be regarded as a success are different for different groups. This makes life exciting for the researcher but dangerous for the reviewer. You should know at the start that I work in this area, and that I am as prejudiced as anyone else in the field.)

The slow approach to scaling presents a practical problem for QCD simulations, since it means that one needs to work at small lattice spacing. This is expensive. The cost of a Monte Carlo simulation in a box of physical size L with lattice spacing a and quark mass m_q scales roughly as

$$(\frac{L}{a})^4(\frac{1}{a})^{1-2}(\frac{1}{m_q})^{2-3} \tag{100}$$

where the 4 is just the number of sites, the 1-2 is the cost of "critical slowing down"–the extent to which successive configurations are correlated, and the 2-3 is the cost of inverting the fermion propagator, plus critical slowing down from the nearly massless pions. The problem is that one needs a big computer to do anything.

However, all the simulations I described in the last lecture were done with a particular choice of lattice action: the plaquette gauge action, and either Wilson or staggered quarks. While those actions are the simplest ones to

program, they are just particular arbitrary choices of bare actions. Can one invent a better lattice discretization, which has smaller scaling violations?

To approach this problem, let's think about the connection between scaling and the properties of some arbitrary bare action, which we assume is defined with some UV cutoff a (which does not have to be a lattice cutoff, in principle). The action is characterized by an infinite number of coupling constants, $\{g\}$. When the g's have any arbitrary value, the typical scale for all physics will be the order of the cutoff: $m \simeq 1/a$, correlation length $\xi \simeq a$. There will be strong cutoff effects.

The best way to think about scaling is through the renormalization group [27]. Take the action with cutoff a and integrate out degrees of freedom to construct a new effective action with a new cutoff $a' > a$ and fewer degrees of freedom. The physics at distance scales $r > a$ is unaffected by the coarse-graining (assuming it is done exactly.) We can think of the effective actions as being similar to the original action, but with altered couplings. We can repeat this coarse-graining and generate new actions with new cutoffs. As we do, the coupling constants "flow:"

$$S(a, c_j) \to S(2a, c'_j) \to S(4a, c''_j) \to \dots \tag{101}$$

If under repeated blockings the system flows to a fixed point

$$S(a_n, c_j^n) \to S(a_{n+1}, c_j^{n+1} = c_j^n) \tag{102}$$

then observables are independent of the cutoff a and in particular the correlation length ξ must either be zero or infinite.

This can only happen if the original c's belong to a particular restricted set, called the "critical surface." It is easy to see that physics on the critical surface is universal: at long distances the effective theory is the action at the fixed point, to which all the couplings have flowed, regardless of their original bare values.

But $\xi = \infty$ is not ξ large. Imagine tuning bare parameters close to the critical surface, but not on it. The system will flow towards the fixed point, then away from it. The flow lines in coupling constant space will asymptotically approach a particular trajectory, called the renormalized trajectory, which connects (at $\xi = \infty$) with the fixed point. Along the renormalized trajectory, ξ is finite. However, because it is connected to the fixed point, it shares the scaling properties of the fixed point–in particular, the complete absence of cutoff effects in the spectrum and in Green's functions. (To see this remarkable result, imagine doing QCD spectrum calculations with the original bare action with a cutoff equal to the Planck mass-or beyond (!) and then coarse graining.

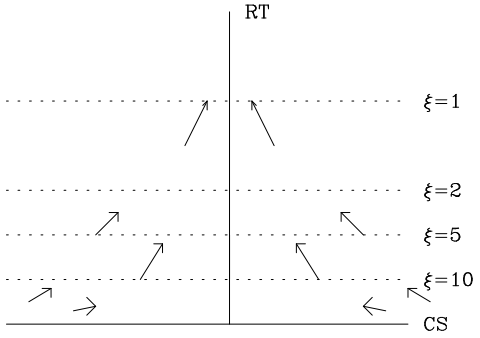

Figure 11: A schematic picture of renormalization group flows along a one-dimensional critical surface, with the associated renormalized trajectory, and superimposed contours of constant correlation length.

Now exchange the order of the two procedures. If this can be done without making any approximations the answer should be the same.)

A Colorado analogy is useful: think of the critical surface as the top of a high mountain ridge. The fixed point is a saddle point on the ridge. A stone released on the ridge will roll to the saddle and come to rest. If it is not released exactly on the ridge, it will roll near to the saddle, then go down the gully leading away from it. For a cartoon, see Fig. 11.

So the ultimate goal of "improvement programs" is to find a true perfect action, without cutoff effects, along the renormalized trajectory of some renormalization group transformation.

The bare action for an asymptotically free theory like QCD can be characterized by one weakly relevant operator, $F_{\mu\nu}^2$, and its associated coupling g^2, plus many irrelevant operators. In lattice language, our bare actions are described by one overall factor of $\beta = 2N/g^2$ and arbitrary weights of various closed loops,

$$\beta S = \frac{2N}{g^2} \sum_j c_j O_j. \tag{103}$$

Asymptotic freedom is equivalent to the statement that the critical surface of any renormalization group transformation is at $g^2 = 0$. The location of a fixed

point involves some relation among the c_j's.

As you might imagine, finding a renormalized trajectory is hard, and nobody has done it in a convincing way yet for QCD. What are people doing in the meantime?

6.1 Improvement based on naive dimensional analysis

The idea here is that since the critical surface is at $g^2 \to 0$ we can use the naive canonical dimensionality of operators to guide us in our choice of improvement. If we perform a naive Taylor expansion of a lattice operator like the plaquette, we find that it can be written as

$$\begin{aligned} 1 - \frac{1}{3}\text{Re Tr}U_{plaq} = \quad & r_0 \text{Tr} F_{\mu\nu}^2 + a^2 [r_1 \textstyle\sum_{\mu\nu} \text{Tr} D_\mu F_{\mu\nu} D_\mu F_{\mu\nu} + \\ & r_2 \textstyle\sum_{\mu\nu\sigma} \text{Tr} D_\mu F_{\nu\sigma} D_\mu F_{\nu\sigma} + \\ & r_3 \textstyle\sum_{\mu\nu\sigma} \text{Tr} D_\mu F_{\mu\sigma} D_\nu F_{\nu\sigma}] + \\ & + O(a^4) \end{aligned} \tag{104}$$

The expansion coefficients have a power series expansion in the coupling, $r_j = A_j + g^2 B_j + \ldots$ and the expectation value of any operator T will have an expansion

$$\langle T(a) \rangle = \langle T(0) \rangle + O(a) + O(g^2 a) + \ldots \tag{105}$$

Other loops have a similar expansion, with different coefficients. Now the idea is to take a minimal subset of loops and systematically remove the a^n terms order by order for physical observables by taking the right linear combination of loops.

$$S = \sum_j c_j O_j \tag{106}$$

with

$$c_j = c_j^0 + g^2 c_j^1 + \ldots \tag{107}$$

"Tree level" improvement removes pure power-law corrections through some order in a^n. One can also consider quantum corrections, and at each order in a^n remove g^m terms, too. This method was developed by Symanzik and co-workers [28] [29] [30] ten years ago.

The most commonly used "improved" fermion action is the "Sheikholeslami-Wohlert" [31] or "clover" action, an order a^2 improved Wilson action. The original Wilson action has $O(a)$ errors in its vertices, $S_W = S_c + O(a)$. This is corrected by making a field redefinition

$$\psi(x) \to \psi'(x) = \quad \psi(x) + \tfrac{ia}{4} \gamma_\mu D_\mu \psi \tag{108}$$

$$\bar{\psi}(x) \to \bar{\psi}'(x) = \quad \bar{\psi}(x) + \tfrac{ia}{4} \gamma_\mu \bar{\psi} D_\mu \tag{109}$$

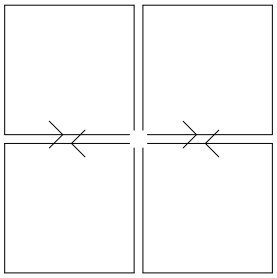

Figure 12: The "clover term".

and the net result is an action with an extra lattice anomalous magnetic moment term,

$$S_{SW} - \frac{iag}{4}\bar{\psi}(x)\sigma_{\mu\nu}F_{\mu\nu}\psi(x) \tag{110}$$

It is called the "clover" action because the lattice version of $F_{\mu\nu}$ is the sum of paths shown in Fig. 12.

Studies performed at the time showed that this program did not improve scaling for the pure gauge theory (in the sense that the cost of simulating the more complicated action was greater than the savings from using a larger lattice spacing.) The whole program was re-awakened in the last few last years by Lepage and collaborators [32] and variations of this program give the most widely used "improved" lattice actions.

6.2 Nonperturbative determination of coefficients

Although I am breaking chronological order, the simplest approach to Symanzik improvement is the newest. The idea [33] is to force the lattice to obey various desirable identities to some order in a, by tuning parameters until the identities are satisfied by the simulations. Then calculate other things. One example is the PCAC relation

$$\partial_\mu A^a_\mu = 2m^a_P + O(a), \tag{111}$$

where the axial and pseudoscalar currents are just

$$A_\mu^a(x) = \bar{\psi}(x)\gamma_\mu\gamma_5\frac{1}{2}\tau^a\psi(x) \tag{112}$$

and

$$P^a(x) = \bar{\psi}(x)\gamma_5\frac{1}{2}\tau^a\psi(x) \tag{113}$$

(τ^a is an isospin index.) The PCAC relation for the quark mass is

$$m \equiv \frac{1}{2}\frac{\langle\partial_\mu A_\mu^a O^a\rangle}{\langle P^a O^a\rangle} + O(a). \tag{114}$$

Now the idea is to take some Symanzik-improved action, with the expansion coefficients allowed to vary, and perform simulations in a little box with some particular choice of boundary conditions for the fields. Tune the parameters, which include the $i/4c_{SW}a\sigma_{\mu\nu}F_{\mu\nu}$ and redefined currents

$$A_\mu = Z_A[(1 + b_A a m_q)A_\mu^a + c_A a\partial_\mu P^a \tag{115}$$

$$P^a = Z_P(1 + b_P a m_q)P^a, \tag{116}$$

until the quark mass, defined in Eq. 114, is independent of location in the box, or of the boundary conditions. Figs. 13 and 14 illustrate what can be done with this tuning procedure. It is still too soon for definitive tests of scaling with this procedure.

6.3 Improving perturbation theory

The older version of Symanzik improvement uses lattice perturbation theory to compute the coefficients of the operators in the action. Let's make a digression into lattice perturbation theory [34]. It has three major uses. First, we need to relate lattice quantities (like matrix elements) to continuum ones: $O^{cont}(\mu) = Z(\mu a, g(a))O^{latt}(a)$. This happens because the renormalization of an operator is slightly different in the two schemes. In perturbation theory Z has an expansion in powers of g^2. Second, we can use perturbation theory to understand and check numerical calculations when the lattice couplings are very small. Finally, one can use perturbative ideas to motivate nonperturbative improvement schemes [35].

Perturbation theory for lattice actions is just like any other kind of perturbation theory (only much messier). One expands the Lagrangian into a

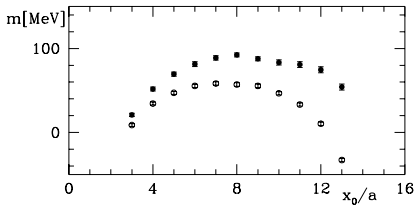

Figure 13: Values of the quark mass as computed from the axial and pseudoscalar currents, using the Wilson action. The open and full symbols correspond to different boundary conditions on the gauge fields.

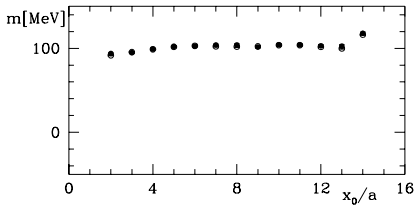

Figure 14: Same as previous figure, but now with improved action and operators.

quadratic term and interaction terms and constructs the propagator from the quadratic terms:

$$\begin{aligned} \mathcal{L} = &\quad A_\mu(x)\rho_{\mu\nu}(x-y)A_\nu(y) + gA^3 + \ldots \quad (117) \\ = &\quad \mathcal{L}_0 + \mathcal{L}_I. \quad (118) \end{aligned}$$

For example, the gluon propagator in Feynman gauge for the Wilson action is

$$D_{\mu\nu}(q) = \frac{g_{\mu\nu}}{\sum_\mu (1-\cos(q_\mu a))}. \quad (119)$$

To do perturbation theory for any system (not just the lattice) one has to do three things: one has to fix the renormalization scheme (RS) (define a coupling), specify the scale at which the coupling is defined, and determine a numerical value for the coupling at that scale. All of these choices are arbitrary, and any perturbative calculation is intrinsically ambiguous.

Any object which has a perturbative expansion can be written

$$O(Q) = c_0 + c_1(Q/\mu, RS)\alpha_s(\mu, RS) + c_2(Q/\mu, RS)\alpha_s(\mu, RS)^2 + \ldots \quad (120)$$

In perturbative calculations we truncate the series after a fixed number of terms and implicitly assume that's all there is. The coefficients $c_i(Q/\mu, RS)$ and the coupling $\alpha_s(\mu, RS)$ depend on the renormalization scheme and choice of scale μ. The guiding rule of perturbation theory [34] is "For a good choice of expansion the uncalculated higher order terms should be small." A bad choice has big coefficients.

There are many ways to define a coupling: The most obvious is the bare coupling; as we will see shortly, it is a poor expansion parameter. Another possibility is to define the coupling from some physical observable. One popular choice is to use the heavy quark potential at very high momentum transfer to define

$$V(q) \equiv 4\pi C_f \frac{\alpha_V(q)}{q^2}. \quad (121)$$

There are also several possibilities for picking a scale: One can use the bare coupling, then $\mu = 1/a$ the lattice spacing. One can guess the scale or or play games just like in the continuum. One game is the Lepage-Mackenzie q^* prescription: take

$$\alpha_s(q^*) \int d^4q \xi(q) = \int d^4q \xi(q) \alpha_s(q). \quad (122)$$

To find q^*, write $\alpha_s(q) = \alpha_s(\mu) + b\ln(q^2/\mu^2)\alpha_s(\mu)^2 + \ldots$, and similarly for $\alpha_s(q^*)$, insert these expressions into Eq. 122 and compare the $\alpha_s(\mu)^2$ terms,

to get

$$\ln(q^*) = \int d^4q \ln(q)\xi / \int d^4q\xi. \tag{123}$$

This is the lattice analog of the Brodsky-Lepage-Mackenzie [37] prescription in continuum PT.

Finally one must determine the coupling: If one uses the bare lattice coupling it is already known. Otherwise, one can compute it in terms of the bare coupling:

$$\alpha_{\overline{MS}}(s/a) = \alpha_0 + (5.88 - 1.75\ln s)\alpha_0^2 + (43.41 - 21.89\ln s + 3.06\ln^2 s)\alpha_0^3 + \ldots \tag{124}$$

Or one can determine it from something one measures on the lattice, which has a perturbative expansion. For example

$$-\ln\langle\frac{1}{3}\mathrm{Tr}U_{plaq}\rangle = \frac{4\pi}{3}\alpha_P(3.41/a)(1 - 1.185\alpha_P) \tag{125}$$

(to this order, $\alpha_P = \alpha_V$). Does "improved perturbation theory" actually improve perturbative calculations? In many cases, yes: some examples are shown in Fig. 15 from [35]: On the upper left we see a calculation of the average link in Landau gauge, from simulations (octagons) and then from lowest-order perturbative calculations using the bare coupling (crosses) and α_V and $\alpha_{\bar{M}S}$ (diamonds and squares). In the upper right panel we see how the lattice prediction of an observable involving the 2 by 2 Wilson loop depends on the choice of momentum q^*/a (at $\beta = 6.2$, a rather weak value of the bare coupling) in the running coupling constant. The burst is the value of the prescription of Eq. 123. In the lower panel are perturbative predictions the same observables as a function of lattice coupling. These pictures illustrate that perturbation theory in terms of the bare coupling does not work well, but that using other definitions for couplings, one can get much better agreement with the lattice "data".

Straight perturbative expansions by themselves for the commonly-used lattice actions are typically not very convergent. The culprit is the presence of U_μ's in the action. One might think that for weak coupling, one could expand

$$\bar{\psi}U\psi = \bar{\psi}[1 + igaA + \ldots]\psi \tag{126}$$

and ignore the ..., but the higher order term $\bar{\psi}\frac{1}{2}g^2a^2A^2\psi$ generates the "tadpole graph" of Fig. 16. The UV divergence in the gluon loop $\simeq 1/a^2$ cancels the a^2 in the vertex. The same thing happens at higher order, and the tadpoles add up to an effective $a^0\sum c_n g^{2n}$ contribution. Parisi [36] and later Lepage and Mackenzie [35] suggested a heuristic way to deal with this problem: replace

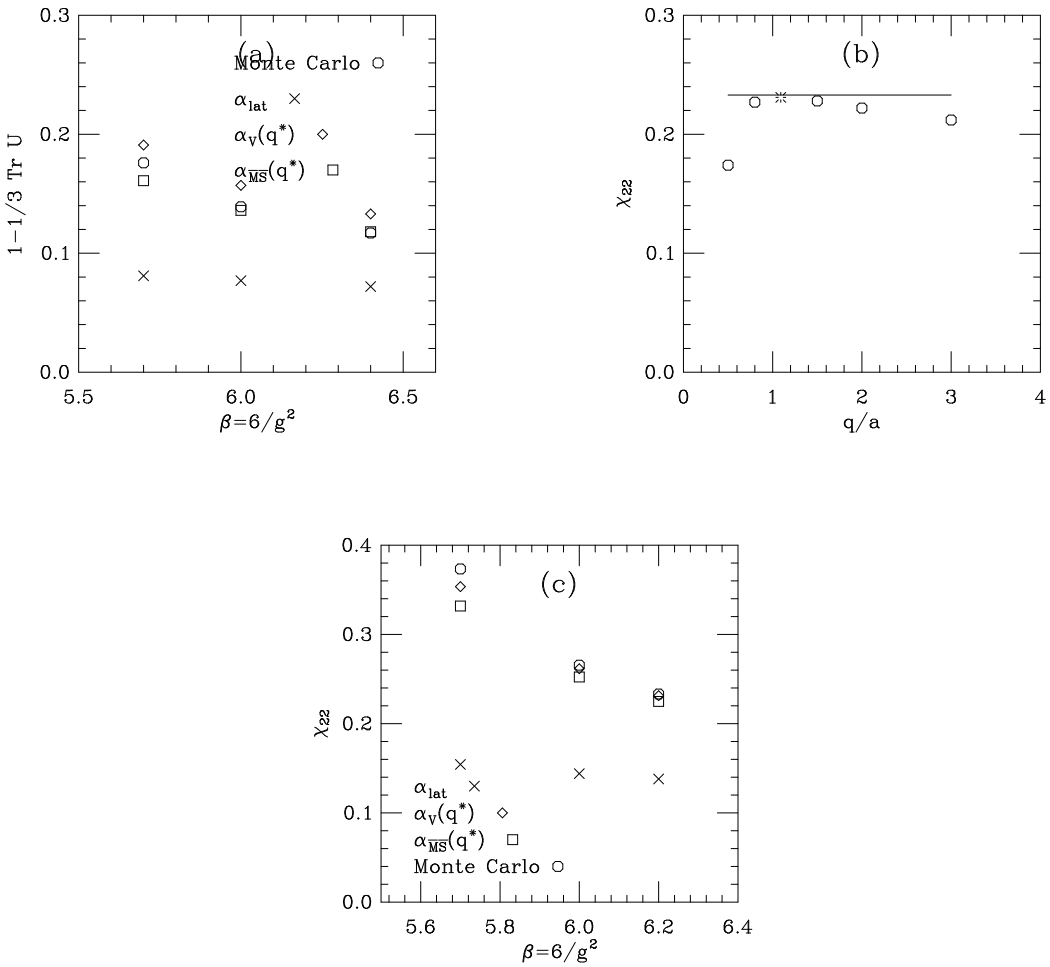

Figure 15: Examples of "improved perturbation theory".

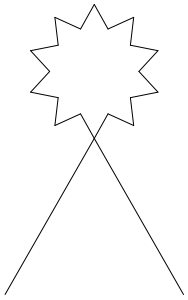

Figure 16: The "tadpole diagram".

$U_\mu \to u_0(1+igaA)$ where u_0, the "mean field term" or "tadpole improvement term" is introduced phenomenologically to sum the loops. Then one rewrites the action as

$$S = \frac{1}{g^2 u_0^4} \sum \mathrm{Tr}U \leftrightarrow \frac{1}{g_{lat}^2} \sum \mathrm{TrU} \tag{127}$$

where $g^2 \equiv g_{lat}^2/u_0^4$ is the new expansion parameter. Is $u_0^4 \equiv \langle \mathrm{Tr}U_{plaq}/3 \rangle$? This choice is often used; it is by no means unique.

A "standard action" (for this year, anyway) is the "tadpole-improved Lüscher-Weisz [30] action," composed of a 1 by 1, 1 by 2, and "twisted" loop (+x,+y,+z,-x,-y,-z),

$$\beta S = -\beta[\mathrm{Tr}(1\times 1) - \frac{1}{20u_0^2}(1+0.48\alpha_s)\mathrm{Tr}(1\times 2) - \frac{1}{u_0^2}0.33\alpha_s \mathrm{Tr}U_{tw}] \tag{128}$$

with $u_0 \equiv \langle \mathrm{Tr}U_{plaq}/3 \rangle^{1/4}$ and $3.068\alpha_s \equiv -\ln\langle \mathrm{Tr}U_{plaq}/3 \rangle$ determined self-consistently in the simulation.

None of this section seems to have anything to do with critical surfaces or renormalized trajectories. What is going on? I believe that the connection is that people following this path to improvement are (implicitly) trying to find a trajectory in coupling constant space for which physical observables have no cutoff effects through some order in a^n and/or $(g^2)^m a^n$. The trajectory is described by the variation of the c_j's in Eqn. 106 with respect to a or to

bare g^2. If perturbation theory is reliable, one could compute them using the expansion of Eqn. 107. This is not a renormalized trajectory, but it might be "good enough" in the engineering sense.

6.4 Fixed Point Actions

A more direct attack on the renormalized trajectory begins by finding a fixed point action. Imagine having a set of field variables $\{\phi\}$ defined with a cutoff a. Introduce some coarse-grained variables $\{\Phi\}$ defined with respect to a new cutoff a', and integrate out the fine-grained variables to produce a new action

$$\mathrm{e}^{-\beta S'(\Phi)} = \int d\phi \mathrm{e}^{-\beta(T(\Phi,\phi)+S(\phi))} \tag{129}$$

where $\beta(T(\Phi,\phi)$ is the blocking kernel which functionally relates the coarse and fine variables. Integrating Eq. 129 is usually horribly complicated. However, P. Hasenfratz and F. Niedermayer [38] noticed an amazing simplification for asymptotically free theories: Their critical surface is at $\beta = \infty$ and in that limit Eq. 129 becomes a steepest-descent relation

$$S'(\Phi) = \min_{\phi}((T(\Phi,\phi) + S(\phi)) \tag{130}$$

which can be used to find the fixed point action

$$S_{FP}(\Phi) = \min_{\phi}((T(\Phi,\phi) + S_{FP}(\phi)). \tag{131}$$

The program has been successfully carried out for $d = 2$ sigma models [38] and for four-dimensional pure gauge theories [39]. These actions have two noteworthy properties: First, not only are they classically perfect actions (they have no a^n scaling violations for any n), but they are also one-loop quantum perfect: that is, as one moves out the renormalized trajectory,

$$\frac{1}{g^2} S_{RT}(g^2) = \frac{1}{g^2}(S_{FP} + O(g^4)). \tag{132}$$

Physically this happens because the original action has no irrelevant operators, and they are only generated through loop graphs. Thus these actions are an extreme realization of the Symanzik program. Second, because these actions are at the fixed point, they have scale invariant classical solutions. This fact can be used to define a topological charge operator on the lattice in a way which is consistent with the lattice action [40].

These actions are "engineered" in the following way: one picks a favorite blocking kernel, which has some free parameters, and solves Eq. 131, usually approximately at first. Then one tunes the parameters in the kernel to optimize the action for locality, and perhaps refines the solution. Now the action is used in simulations at finite correlation length (i.e. do simulations with a Boltzman factor $\exp(-\beta S_{FP})$. Because of Eq. 132, one believes that the FP action will be a good approximation to the perfect action on the RT; of course, only a numerical test can tell. As we will see in the next section, these actions perform very well. At this point in time no nonperturbative FP action which includes fermions has been tested, but most of the formalism is there [41].

6.5 Examples of "Improved" Spectroscopy

I would like to show some examples of the various versions of "improvement", and remind you of the pictures at the end of the last chapter to contrast results from standard actions.

Fig. 17 shows a plot of the string tension measured in systems of constant physical size (measured in units of $1/T_c$, the critical temperature for deconfinement), for SU(3) pure gauge theory. In the quenched approximation, with $\sqrt{\sigma} \simeq 440$ MeV, $T_c = 275$ MeV and $1/T_c = 0.7$ fm. Simulations with the standard Wilson action are crosses, while the squares show FP action results [39] and the octagons from the tadpole-improved Lüscher-Weisz action [42]. The figure illustrates that it is hard to quantify improvement. There are no measurements with the Wilson action at small lattice spacing of of precisely the same observables that the "improvement people" measured. The best one can do is to take similar measurements (the diamonds) and attempt to compute the $a = 0$ prediction for the observable we measured (the fancy cross at $a = 0$). This attempt lies on a straight line with the FP action data, hinting strongly that the FP action is indeed scaling. The FP action seems to have gained about a factor of three to four in lattice spacing, or a gain of $(3-4)^6$ compared to the plaquette action, according to Eq. 100, at a cost of a factor of 7 per site because it is more complicated to program. The tadpole-improved Lüscher-Weisz action data lie lower than the FP action data and do not scale as well. As $a \to 0$ the two actions should yield the same result; that is just universality at work. However, there is no guarantee that the approach to the continuum is monotonic.

Fig. 18 shows the heavy quark-antiquark potential in SU(2) gauge theory, where $V(r)$ and r are measured in the appropriate units of T_c, the critical temperature for deconfinement. The Wilson action is on the left and a FP action is on the right. The vertical displacements of the potentials are just

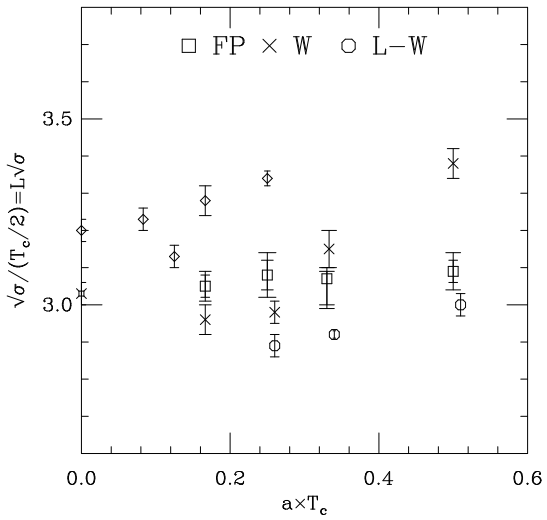

Figure 17: The (square root of) the string tension in lattices of constant physical size $L = 2/T_c$, but different lattice spacings (in units of $1/T_c$).

there to separate them. Notice the large violations of rotational symmetry in the Wilson action data when the lattice spacing is $a = 1/2T_c$ which are considerably improved in the FP action results.

Next we consider nonrelativistic QCD. A comparison of the quenched charmonium spectrum from Ref. [32] is shown in Fig. 19. When the tadpole-improved L-W action is used to generate gauge configurations, the scaling window is pushed out to $a \simeq 0.4$ fm for these observables.

Now we turn to tests of quenched QCD for light quarks. The two actions which have been most extensively tested are the S-W action, with and without tadpole improvement, and an action called the D234(2/3) action, a higher-order variant of the S-W action [44]. Figs. 20 and 21, are the analogs of Figs. 8 and 9. Diamonds [45] and plusses [46] are S-W actions, ordinary and tadpole-improved, squares are the D234(2/3) action. They appear to have about half the scaling violations as the standard actions but they don't remove all scaling violations. It's a bit hard to quantify the extent of improvement from these pictures because a chiral extrapolation is hidden in them. However, one can take one of the "sections" of Fig. 7 and overlay the new data on it, Fig. 22. It looks like one can double the lattice spacing for an equivalent amount of scale violation. However, the extrapolation in a is not altogether clear. Fig. 23 is the same data as Fig. 22, only plotted vs. a^2, not a. All of the actions shown

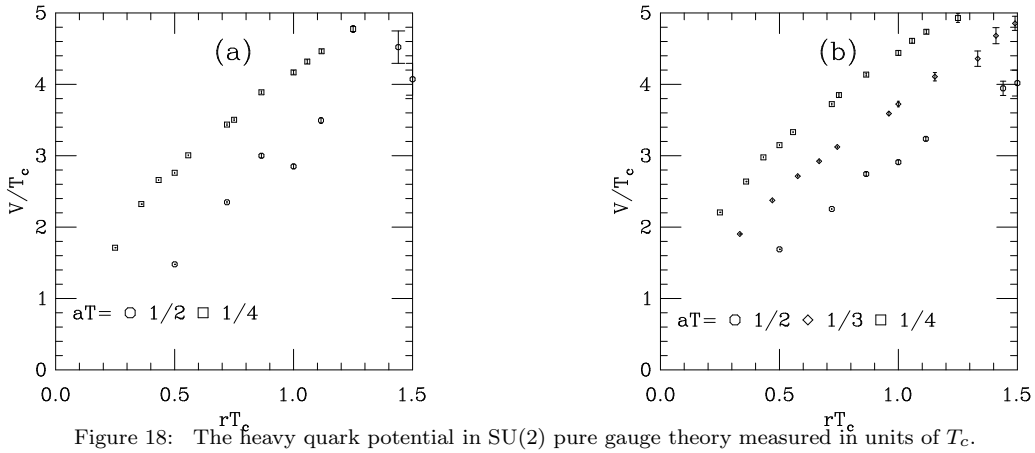

Figure 18: The heavy quark potential in SU(2) pure gauge theory measured in units of T_c. (a) Wilson action (b) an FP action.

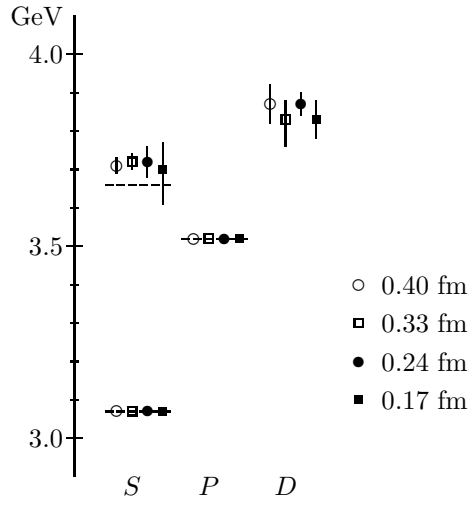

Figure 19: S, P, and D states of charmonium computed on lattices with: $a = 0.40$ fm (improved action, $\beta_{plaq} = 6.8$); $a = 0.33$ fm (improved action, $\beta_{plaq} = 7.1$); $a = 0.24$ fm (improved action, $\beta_{plaq} = 7.4$); and $a = 0.17$ fm (Wilson action, $\beta = 5.7$, from [43]), from Ref. 32. The dashed lines indicate the true masses.

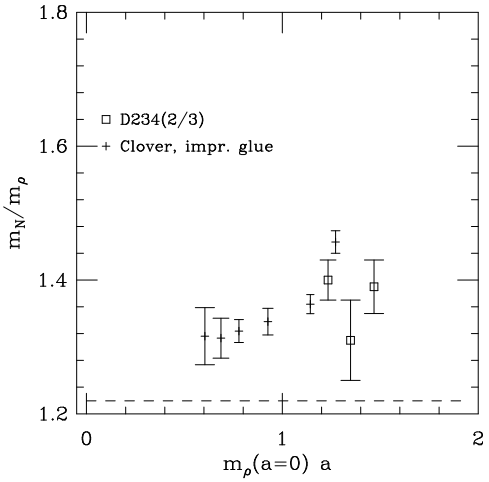

Figure 20: Nucleon to rho mass ratio (at chiral limit) vs. lattice spacing (in units of $1/m_\rho$).

in these figures are supposed to have $O(a^2)$ (or better) scaling violations. Do the data look any straighter in Fig. 23 than Fig. 22?

6.6 The bottom line

At the cost of enormous effort, one can do fairly high precision simulations of QCD in the quenched approximation with standard actions. The actions I have shown you appear to reduce the amount of computation required for pure gauge simulations from supercomputers to very large work stations, probably a gain of a few hundreds. All of the light quark data I showed actually came from supercomputers. According to Eq. 100, a factor of 2 in the lattice spacing gains a factor of 64 in speed. The cost of either of the two improved actions I showed is about a factor of 8-10 times the fiducial staggered simulation. Improvement methods for fermions are a few years less mature than ones for pure gauge theory, and so the next time you hear a talk about the lattice, things will have changed for the better (maybe).

7 Case Studies

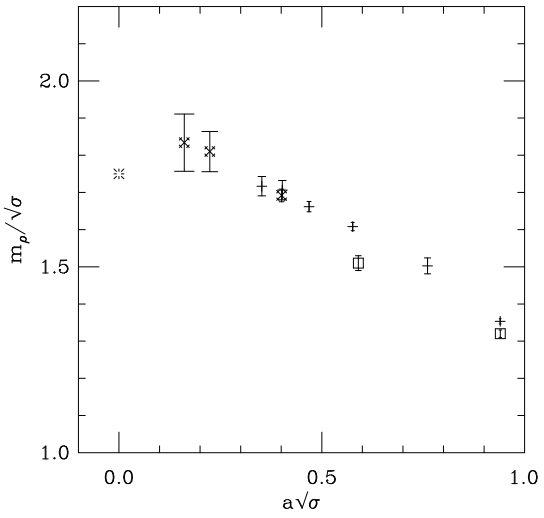

Figure 21: Rho mass scaling test with respect to the string tension.

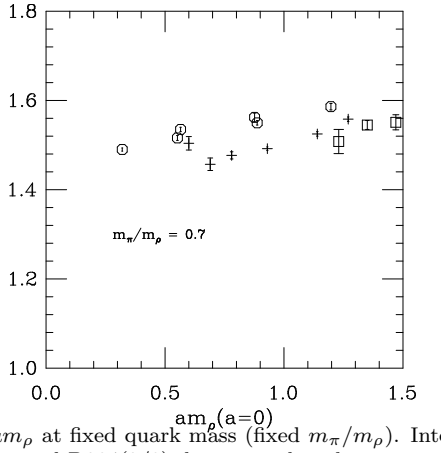

Figure 22: m_N/m_ρ vs am_ρ at fixed quark mass (fixed m_π/m_ρ). Interpolations of the S-W and D234(2/3) data were done by me.

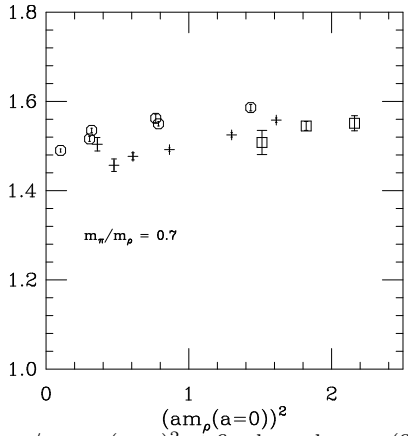

Figure 23: m_N/m_ρ vs $(am_\rho)^2$ at fixed quark mass (fixed m_π/m_ρ).

7.1 Glueballs

To this audience, glueballs are just the closed strings of QCD. They are interesting because they are part of the QCD spectrum but not part of a naive quark model. What do we expect for a spectrum? Models like the bag model, which have bound "constituent gluons," would predict that the lightest state is a scalar, followed by tensor and pseudoscalar states, but nobody really knows. Here is a place where the lattice is the only game in town for a first-principles calculation.

Since this is a TASI for stringy graduate students, the experimental situation can be summarized briefly: it is a mess [47]. There are two leading experimental candidates, the $f_J(1700)$, seen in radiative ψ decays ($\psi \to \gamma K\bar{K}$ and $\psi \to \gamma\eta\eta$ (mostly at SLAC)) and the $f_0(1500)$, seen in $p\bar{p} \to \pi^0\eta\eta$, from the Crystal Barrel detector at CERN.

People have been trying to measure the masses of the lightest glueballs (the scalar and the tensor) using lattice simulations for many years. The problem has proven to be very hard, for several reasons.

Recall how we measure a mass from a correlation function (Eqn. 99). The problem with the scalar glueball is that the operator O has nonzero vacuum expectation value, and the correlation function approaches a constant at large

t:

$$\lim_{t\to\infty} C(t) \to |\langle 0|O|\vec{p}=0\rangle|^2 \exp(-mt) + |\langle 0|O|0\rangle|^2. \tag{133}$$

The statistical fluctuations on $C(t)$ are given by Eq. 90 and we find after a short calculation that

$$\sigma \to \frac{C(0)}{\sqrt{N}}. \tag{134}$$

Thus the signal to noise ratio collapses at large t like $\sqrt{N}\exp(-mt)$ due to the constant term.

A partial cure for this problem is a good trial wave function O. While in principle the plaquette itself could be used, it is so dominated by ultraviolet fluctuations that it does not produce a good signal. Instead, people invent "fat links" which average the gauge field over several lattice spacings, and then make interpolating fields which are closed loops of these fat links. The lattice glueball is a smoke ring.

The second problem is that lattice actions can have phase transitions at strong or intermediate coupling, which have nothing to do with the continuum limit, but mask continuum behavior [48]. As an example of this, consider the gauge group $SU(2)$, where a link matrix can be parameterized as $U = 1\cos\theta + i\vec{\sigma}\cdot\vec{n}\sin\theta$, so $\mathrm{Tr}U = 2\cos\theta$. Now consider a generalization of the Wilson action $-S = \beta\mathrm{Tr}U + \gamma(\mathrm{Tr}U)^2$. (this is a mixed fundamental-adjoint representation action). At $\gamma \to \infty$ $\mathrm{Tr}U \to \pm 1$ and the gauge symmetry is broken down to $Z(2)$. But $Z(2)$ gauge theories have a first order phase transition. First order transitions are stable under perturbations, and so the phase diagram of this theory, shown in Fig. 24, has a line of first order transitions which terminate in a second order point. At the second order point some state with scalar quantum numbers becomes massless. However, now imagine that you are doing Monte Carlo along the $\gamma = 0$ line, that is, with the Wilson action. When you come near the critical point, any operator which couples to a scalar particle (like the one you are using to see the scalar glueball) will see the nearby transition and the lightest mass in the scalar channel will shrink. Once you are past the point of closest approach, the mass will rise again. Any scaling test which ignores the nearby singularity will lie to you.

This scenario has been mapped out for $SU(3)$, and the place of closest approach is at a Wilson coupling corresponding to a lattice spacing of 0.2 fm or so, meaning that very small lattice spacings are needed before one can extrapolate to zero lattice spacing. A summary of the situation is shown in Fig. 25 [49]. Here the quantity r_0 is the "Sommer radius" [50], defined through the force, by $r_0^2 F(r_0) = -1.65$. In the physical world of three colors and four flavors, $r_0 = 0.5$ fm.

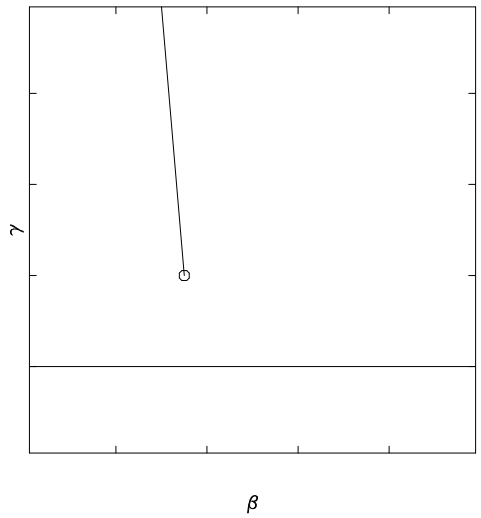

Figure 24: Phase transitions in the fundamental-adjoint plane.

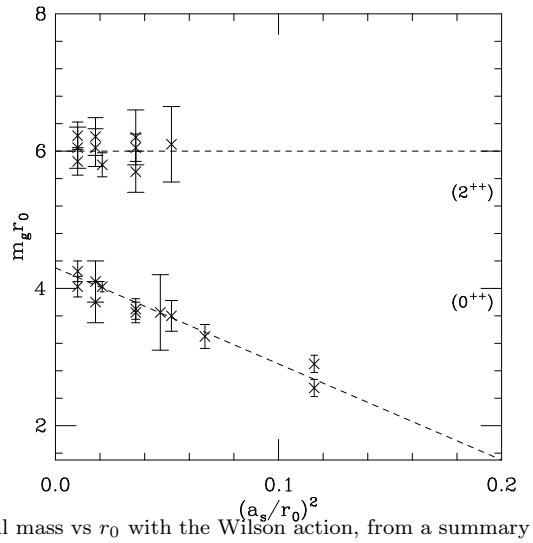

Figure 25: Glueball mass vs r_0 with the Wilson action, from a summary picture in Ref. 49.

Finally, other arguments suggest that a small lattice spacing or a good approximation to an action on an RT are needed to for glueballs: the physical diameter of the glueball, as inferred from the size of the best interpolating field, is small, about 0.5 fm. Shäfer and Shuryak [51] have argued that the small size is due to instanton effects. Most lattice actions at large lattice spacing do bad things to instantons [40].

Two big simulations have carried calculations of the glueball mass close to the continuum limit: the UKQCD collaboration [52] and a collaboration at IBM which built its own computer [53]. (The latter group is the one with the press release last December announcing the discovery of the glueball.) Their predictions in MeV are different and they each favor a different experimental candidate for the scalar glueball (the one which is closer to their prediction, of course). It is a useful object lesson because both groups agree that their lattice numbers agree before extrapolation, but they extrapolate differently to $a = 0$.

The UKQCD group sees that the ratio $m(0^{++})/\sqrt{\sigma}$ can be well fitted with a form $b + ca^2\sigma$ (σ is the string tension) and a fit of this form to the lattice data of both groups gives $m(0^{++})/\sqrt{\sigma} = 3.64 \pm 0.15$. To turn this into MeV we need σ in MeV units. One way is to take $m_\rho/\sqrt{\sigma}$ and extrapolate that to $a = 0$ using $b + ca\sqrt{\sigma}$. Averaging and putting 770 MeV for m_ρ one gets $\sqrt{\sigma} = 432 \pm 15$ MeV, which is consistent with the usual estimate (from extracting the string tension from the heavy quark potential) of about 440 MeV. Using the total average they get $m(0^{++}) = 1572 \pm 65 \pm 55$ MeV where the first error is statistical and the second comes from the scale.

The IBM group, on the other hand, notices that $m_\rho a$ and $m_\phi a$ scale asymptotically, use the phi mass to predict quenched $\Lambda_{\bar{M}S}$, then extrapolate $m(0^{++})/\Lambda = A + B(a\Lambda)^2$. They get 1740(41) MeV from their data, when they analyze UKQCD data, they get 1625(94) MeV, and when they combine the data sets, they get 1707(64) MeV.

A neutral reporter could get hurt here. It seems to me that the lattice prediction for the scalar glueball is 1600 ± 100 MeV, and that there are two experimental candidates for it.

Masses are not the end of the story. The IBM group has done two interesting recent calculations related to glueballs, which strengthen their claim that the $f_J(1710)$ is the glueball.

The first one of them [54] was actually responsible for the press release. It is a calculation of the decay width of the glueball into pairs of pseudoscalars. This is done by computing an unamputated three point function on the lattice, with an assumed form for the vertex, whose magnitude is fitted. The result is shown in Fig. 26. The octagons are the results of the simulation and the

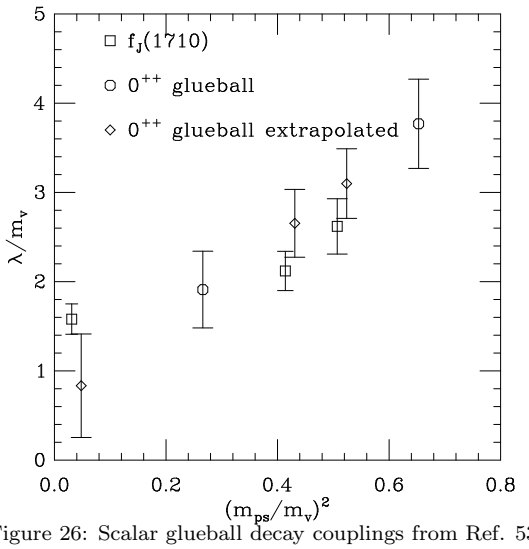

Figure 26: Scalar glueball decay couplings from Ref. 53.

diamonds show interpolations in the quark mass. The "experimental" points (squares) are from a partial wave analysis of isoscalar scalar resonances by Longacre and Lindenbaum [55].

The response of a member of the other side is that the slope of the straight line that one would put through the three experimental points is barely, if at all, compatible with the slope of the theoretical points. Since they argue theoretically for a straight line, the comparison of such slopes is a valid one.

If one of the experimental states is not a glueball, it is likely to be a $^3P_0$ orbital excitation of quarks. Weingarten and Lee [56] are computing the mass of this state on the lattice and argue that it is lighter than 1700 MeV; in their picture the $f_0(1500)$ is an $s\bar{s}$ state. I have now said more than I know and will just refer you to recent discussions of the question [57].

Both groups predict that the 2^{++} glueball is at about 2300 MeV.

Can "improved actions" help the situation? Recently, Peardon and Morningstar [49] implemented a clever method for beating the exponential signal-to-noise ratio: make the lattice spacing smaller in the time direction than in the space direction. Then the signal, which falls like $\exp(-ma_tL_t)$ after L_t lattice spacings, dies more slowly because a_t is reduced. Their picture of the glueball mass vs r_0. is shown in Fig. 27. They are using the tadpole-improved Lüscher-Weisz action. The pessimist notes the prominent dip in the middle of the curve; this action also has a lattice-artifact transition (somewhere); the

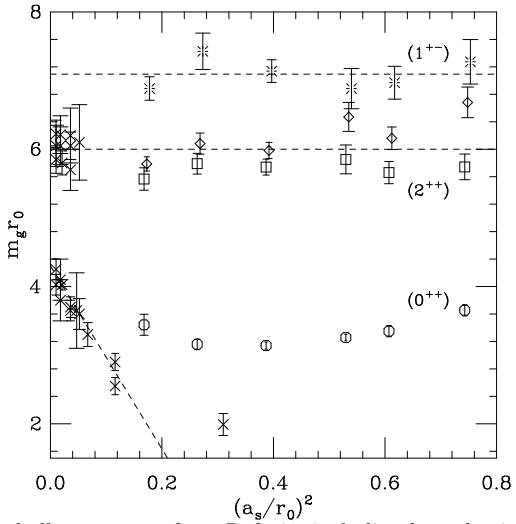

Figure 27: Glueball mass vs r_0 from Ref. 49, including large lattice spacing data.

optimist notes that the dip is much smaller than for the Wilson action and then the pessimist notes that there is no Wilson action data at large lattice spacing to compare. I think the jury is still out.

7.2 $\alpha_s(M_Z)$

For some time now there have been claims that physics at the Z pole hints at a possible breakdown in the standard model[58]. A key question in the discussion is whether or not the value of $\alpha_{\bar{M}S}$ inferred from the decay width of the Z is anomalously high relative to other determinations of the strong coupling (when run to the Z pole, usually).

The most recent analysis I am aware of is due to Erler and Langacker [59]. Currently, $\alpha_{\overline{MS}}^{lineshape} = 0.123(4)(2)(1)$ for the standard model Higgs mass range, where the first/ second/ third uncertainty is from inputs/ Higgs mass/ estimate of α_s^4 terms. The central Higgs mass is assumed to be 300 GeV, and the second error is for $M_H = 1000$ GeV (+), 60 GeV (-). For the SUSY Higgs mass range (60-150 GeV), one has the lower value $\alpha_{\overline{MS}} = .121(4)(+1-0)(1)$. A global fit to all data gives 0.121(4)(1). Hinchcliffe in the same compilation quotes a global average of 0.118(3).

The lattice can contribute to this question by predicting $\alpha_{\overline{MS}}$ from low energy physics. The basic idea is simple: The lattice is a (peculiar) UV cutoff.

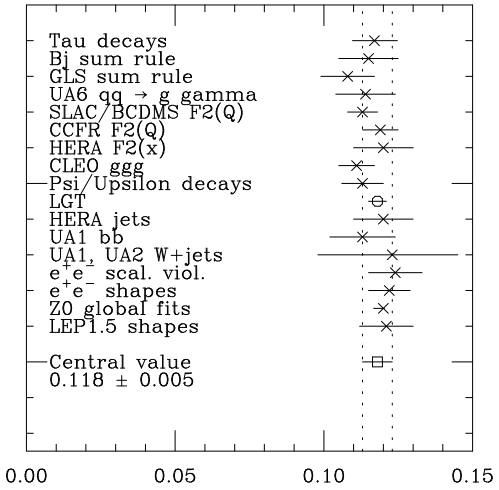

Figure 28: Survey of $\alpha_{\overline{MS}}(M_Z)$ from Ref. 61.

A lattice mass $\mu = Ma$ plus an experimental mass M give a lattice spacing $a = \mu/M$ in fm. If one can measure some quantity related to α_s at a scale $Q \simeq 1/a$, one can then run the coupling constant out to the Z.

The best (recent) lattice number, from Shigemitsu's Lattice 96 summary talk [60], is

$$\alpha_{\overline{MS}}(Z) = 0.1159(19)(13)(19) \tag{135}$$

where the first error includes both statistics and estimates of discretization errors, the second is due to uncertainties from the dynamical quark mass, and the third is from conversions of conventions. The lattice number is about one standard deviation below the pure Z-physics number. Lattice results are compared to other recent determinations of $\alpha_{\overline{MS}}(Z)$ in Fig. 28, a figure provided by P. Burrows [61].

Two ways of calculating $\alpha_s(M_Z)$ from lattice have been proposed: The first is the "small loop method" [62]. This method uses the "improved perturbation theory" described in Chapter 3: One assumes that a version of perturbation theory can describe the behavior of short distance objects on the lattice: in particular, that the plaquette can be used to define $\alpha_V(q = 3.41/a)$. With typical lattice spacings now in use, this gives the coupling at a momentum $Q_0 = 8 - 10$ GeV. One then converts the coupling to $\alpha_{\overline{MS}}$ and runs out to the Z using the (published) three-loop beta function [63].

Usually, the lattice spacing is determined from the mass splittings of heavy

$Q\bar{Q}$ states. This is done because the mass differences between physical heavy quark states are nearly independent of the quark mass– for example, the S-P mass splitting of the ψ family is about 460 MeV, and it is about 440 MeV for the Υ. A second reason is that the mass splitting is believed to be much less sensitive to sea quark effects than light quark observables, and one can estimate the effects of sea quarks through simple potential models. The uncertainty in the lattice spacing is three to five per cent, but systematic effects are much greater (as we will see below).

The coupling constant comes from Eq. 125. The plaquette can be measured to exquisite accuracy (0.01 per cent is not atypical) and so the coupling constant is known essentially without error. However, the scale of the coupling is uncertain (due to the lattice spacing).

The next problem is getting from lattice simulations, which are done with $n_f = 0$ (quenched) or $n_f = 2$ (but unphysical sea quark masses) to the real world of $n_f = 3$. Before simulations with dynamical fermions were available, the translation was done by running down in Q to a "typical gluonic scale" for the psi or the upsilon (a few hundred MeV) and then matching the coupling to the three-flavor coupling (in the spirit of effective field theories). Now we have simulations at $n_f = 2$. Recall that in lowest order

$$\frac{1}{\alpha_s} = \left(\frac{11 - \frac{2}{3}n_f}{4\pi}\right) \ln \frac{Q^2}{\Lambda^2} \tag{136}$$

One measures $1/\alpha_s$ in two simulations, one quenched, the other at $n_f = 2$, runs one measurement in Q to the Q of the other, then extrapolates $1/\alpha$ linearly in n_f to $n_f = 3$. Then one can convert to $\bar{M}S$ and run away.

Pictures like Fig. 28 are not very useful when one wants to get a feel for the errors inherent in the lattice calculation. Instead, let's run our expectations for $\alpha_s(M_Z)$ down to the scale where the lattice simulations are done, and compare. Fig. 29 does that. The squares are the results of simulations of charmed quarks and the octagons are from bottom quarks, both with $n_f = 0$. The crosses and diamond are $n_f = 2$ bottom and charm results. (The bursts show upsilon data when the 1S-2S mass difference gives a lattice spacing.) Note the horizontal error bars on the lattice data. Finally, the predicted $n_f = 3$ coupling α_P is shown in the fancy squares, with error bars now rotated because the convention is to quote an error in α_s. The lower three lines in the picture (from top to bottom) are $\alpha_{\overline{MS}}(M_Z) = 0.118$, 0.123, and 0.128 run down and converted to the lattice prescription.

The two top lines are predictions for how quenched α should run.

Now for the bad news. All of the $n_f = 2$ data shown here were actually run on the same set of configurations. The bare couplings are the same, but the

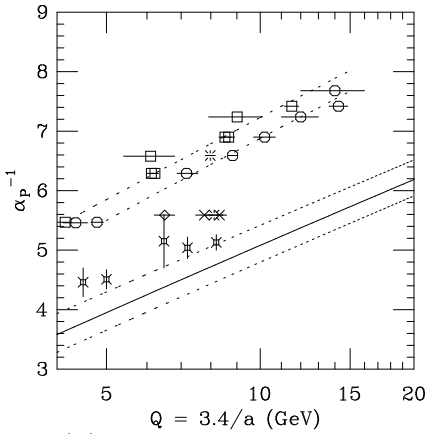

Figure 29: Survey of $\alpha_{\overline{MS}}(Q)$ at the scale where lattice simulations are actually done.

lattice spacings came out different. What is happening is that we are taking calculations at some lattice spacing and inferring a continuum numbers from them, but the lattice predictions have scale violations which are different. (The Υ calculations use nonrelativistic quarks, the ψ calculations use heavy Wilson quarks.) Notice also that the bottom and charm quenched lattice spacings are different. This discrepancy is thought to be a failure of the quenched approximation: the characteristic momentum scale for binding in the ψ and Υ are different, and because n_f is not the real world value α runs incorrectly between the two scales. Said differently, in the quenched approximation, the spectrum of heavy quark bound states is different from the real world.

There is a second method of determining a running coupling constant which actually allows one to see the running over a large range of scales. It goes by the name of the "Schrödinger functional," (referring to the fact that the authors study QCD in a little box with specified boundary conditions) but "coupling determined by varying the box size" would be a more descriptive title. It has been applied to quenched QCD but has not yet been extended to full QCD. I will describe the method in the context of the $d = 2$ sigma model [64] rather than QCD [65].

The idea is that coupling constants can be defined through the response of a system to boundary conditions. For example, if one dimension of a $d = 2$ $O(n)$ sigma model is compactified with size L, the mass gap $M(L)$ (defined

Table 1: Data for the running coupling constant in pure SU(2) gauge theory.

u	$\sigma(2,u)$
2.037	2.45(4)
2.380	2.84(6)
2.840	3.54(8)
3.55	4.76

through the transfer matrix along the other dimension) is related to the coupling through

$$g^2(L) = 2M(L)L/(n-1). \tag{137}$$

The coefficients insure that the answer reduces to the lowest-order result. Now we take take the beta function

$$\beta(g) = L\frac{dg^2}{dL}, \tag{138}$$

stretch the length of the compact dimension from L_0 to sL_0, and compute the change in the coupling

$$\int_{L_0}^{sL_0} \frac{dL}{L} = \int_{g^2(L_0)}^{g^2(sL_0)} \frac{dg^2}{\beta(g^2)} \equiv \int_u^{\sigma(s,u)} \frac{dv}{\beta(v)} \tag{139}$$

where the "step scaling function" $\sigma(s, u = g^2(L)) = g^2(sL)$ is the new coupling constant.

Now the idea is to do simulations with the same bare coupling on systems of size L_0 and sL_0 and, by measuring u and $\sigma(s,u)$, to see how the new coupling depends on the original one. An example of how this works is shown in Table 1. Each horizontal pair are the coupling and its step function (for $s = 2$). The output coupling on the first line is used as the input coupling on the second line (or rather, since these couplings are derived, not bare couplings, one must interpolate to begin with the old output coupling as the new input coupling). When the matching is not perfect, perturbation theory is used for the small amount of running which is required. After four steps the physical length scale has increased by a factor of $2^4 = 16$.

Now we can unfold the couplings. We measure distances in terms of the largest L in the simulation and show the coupling constant in Table 2.

We can introduce a scale in GeV by measuring something physical with the bare parameters corresponding to one of the L's, say, for the gauge theory, the

Table 2: The Schrödinger functional running coupling constant in pure SU(2) gauge theory.

L/L_{max}	$g^2(L)$
1.0	4.765
0.500(23)	3.55
0.249(19)	2.840
0.124(13)	2.380
0.070(8)	2.037

Sommer variable r_0 (it should be obvious why the authors use this observable) at L_{max}. An example of a running coupling constant via this prescription is shown in Fig. 30. This is a coupling constant in a particular prescription; when it is small enough it could be matched to any other prescription using perturbation theory.

All the simulations are done in small lattice volumes. I have left out many technical details, of course. Please note that this calculation checks perturbation theory; it does not use it overtly (apart from the small amount of running I described). I think it is beautiful [66].

8 Conclusions

There it is! I now appreciate what the "string lecturer" goes through when he arrives at TASI's focussed on phenomenology. I have left out a lot. For example, the lattice is a fertile source of numbers for comparisons with the standard model, where what the experimentalist measures is often a combination of a "fundamental parameter" of the standard model times a hadronic matrix element. The lattice and lattice QCD in particular are going through a lot of changes right now, and perhaps for the better. I hope that some of the methods I have described might be useful as a starting point when you find yourselves working in the strong-coupling sector of your favorite theory.

Acknowledgements

I would like to thank M. Alford, P. Burrows, S. Gottlieb, A. Hasenfratz, P. Hasenfratz, U. Heller, P. Langacker, P. Lepage, P. Mackenzie, J. Negele, F. Niedermayer, J. Shigemitsu, J. Simone, R. Sommer, R. Sugar, M. Teper,

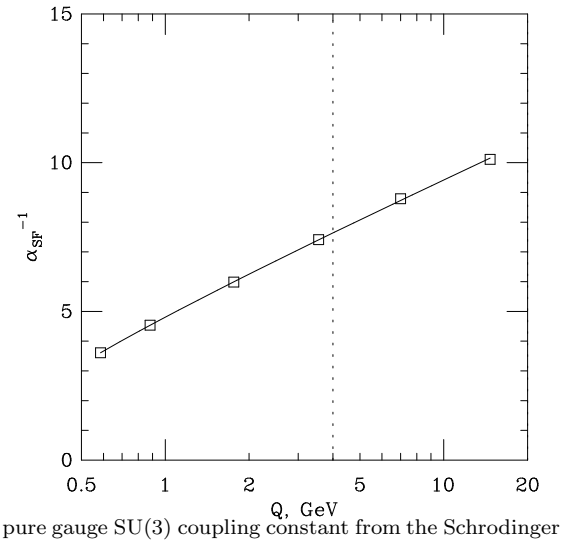

Figure 30: The pure gauge SU(3) coupling constant from the Schrodinger functional method of Ref. 65, with superimposed three-loop prediction. The data from Fig. 29 span the range to the right of the dotted line.

D. Toussaint, D. Weingarten, U. Wiese, and M. Wingate for discussions, figures, and correspondence. They have all influenced these lectures, but probably not in the direction that they intended. I would also like to thank the Institute for Theoretical Physics at the University of Bern for its hospitality, where these lectures were written. This work was supported by the U. S. Department of Energy.

References

1. Some standard reviews of lattice gauge theory are M. Creutz, "Quarks, Strings, and Lattices," Cambridge, 1983. M. Creutz, ed., "Quantum Fields on the Computer," World, 1992, and I. Montvay and G. Munster, "Quantum fields on a lattice," Cambridge, 1994. The lattice community has a large annual meeting and the proceedings of those meetings (Lattice 'XX, published so far by North Holland) are the best places to find the most recent results.
2. K. Wilson, Phys. Rev. D 10, 2445, 1974.
3. M. Creutz, L. Jacobs, C. Rebbi, Phys. Rev. Lett. 42 (1979) 1390.
4. S. Elitzur, Phys. Rev., D12, 3978, 1975.
5. This particular formulation of the problem was shown to me by D. Tou-

ssaint.
6. A good reference for strong coupling expansions is J. M. Drouffe and C. Itzykson, Phys. Rept., 38C, 133, 1978.
7. V. L. Berezinskii, ZhETF (USSR) 59, 907 (1970), (English translation JETP 32, 493 (1971); J. Kosterlitz and D. Thouless, Journal of Physics C6, 1181 (1973); J. Kosterlitz, op. cit. C7, 1046 (1974).
8. J. Jose, L. Kadanoff, S. Kirkpatrick and D. Nelson, Phys. Rev. B16 (1977) 1217.
9. T. Banks, R. Myerson, and J. Kogut, Nucl. Phys. B129 (1977) 493. R. Savit, Phys. Rev. Lett. 39 (1977) 55.
10. A. Polyakov, Nucl. Phys. B120 (1977) 429.
11. T. DeGrand and D. Toussaint, Phys. Rev. D22 (1980) 2478.
12. See W. Franzki, J. Jersak, C. Lang and T. Neuhaus, hep-lat/9607037, hep-lat/9606010 and W. Kerler, C. Rebbi and A. Weber, hep-lat/9607009.
13. See K. Osterwalder and E. Seiler, Ann. Phys. (N. Y.) 110, 440 (1978); E. Fradkin and S. Shenker, Phys. Rev. D19, 3682 (1979).
14. M. Creutz, Phys. Rev. D21, 1006 (1980).
15. For an interesting application, see A. Hasenfratz, P. Hasenfratz, K. Jansen, J. Kuti, and Y. Shen, Nucl. Phys. B365 (1991) 79.
16. M. Golterman and J. Smit, Nucl. Phys., B255, 328, 1985.
17. Cf. G. P. Lepage, in "From Actions to Answers–Proceedings of the 1989 Theoretical Advanced Summer Institute in Particle Physics," T. DeGrand and D. Toussaint, eds., (World, 1990).
18. N. Metropolis, A. Rosenbluth, M. Rosenbluth, A. Teller, and E. Teller, J. Chem. Phys. 21, 1087 (1953).
19. F. Brown and T. Woch, Phys. Rev. Lett., 58, 2394, 1987 ; M. Creutz, Phys. Rev., D36, 55, 1987 . For a review, see S. Adler in the Proceedings of the 1988 Symposium on Lattice Field Theory, A. Kronfeld and P. Mackenzie, eds., (Nucl. Phys. B (Proc. Suppl.) 9 (1989)).
20. H. C. Andersen, J. Chem. Phys., 72, 2384, 1980; S. Duane, Nucl. Phys. B257, 652, 1985; S. Duane and J. Kogut, Phys. Rev. Lett. 55, 2774, 1985; S. Gottlieb, W. Liu, D. Toussaint, R. Renken and R. Sugar, Phys. Rev. D35, 2531, 1987.
21. S. Duane, A. Kennedy, B. Pendleton, and D. Roweth, Phys. Lett. 194B, 271, 1987.
22. For a recent review, see A. Frommer, talk presented at Lattice 96, hep-lat/9608074.
23. E. Shuryak, "Why is a nucleon bound?", hep-ph/9603354, to appear in Festschrift for Gerry Brown's 70.

24. The MILC collaboration, presented at Lattice 96, hep-lat/9608012.
25. F. Butler, et al., Phys. Rev. Lett. 70, (1993) 2849.
26. This plot was kindly provided by R. Sommer.
27. The classic reference is K. Wilson and J. Kogut, Phys. Repts. 12C, 77 (1974).
28. K. Symanzik, in "Recent Developments in Gauge Theories," eds. G. 't Hooft, et al. (Plenum, New York, 1980) 313; in "Mathematical Problems in Theoretical Physics," eds. R. Schrader et al. (Springer, New York, 1982); Nucl. Phys. B226 (1983) 187, 205.
29. P. Weisz , Nucl. Phys. B212 (1983) 1. M. Lüscher and P. Weisz, Comm. Math. Phys. 97, 59 (1985).
30. M. Lüscher and P. Weisz, Phys. Lett. B158, 250 (1985).
31. B. Sheikholeslami and R. Wohlert, Nucl. Phys. B259, 572 (1985).
32. M. Alford, W. Dimm, G. P. Lepage, G. Hockney, and P. Mackenzie, Phys. Lett. B361, 87 (1994) G. P. Lepage, to appear in the Proceedings of Lattice '95, and his Schladming lectures, hep-lat/9607076.
33. K. Jansen, et al., Phys. Lett. B372, 275 1996 (hep-lat/9512009); M. Lüscher, et al., hep-lat/9605038, hep-lat/9608049.
34. C. Morningstar, to appear in the Proceedings of Lattice '95, hep-lat/9509073.
35. G. P. Lepage and P. Mackenzie, Phys. Rev. D48, 2250 (1993).
36. G. Parisi, in High Energy Physics–1980, XX Int. Conf., Madison (1980), ed. L. Durand and L. G. Pondrom (AIP, New York, 1981)
37. S. Brodsky, G. P. Lepage and P. Mackenzie, Phys. Rev. D28, 228 (1983).
38. P. Hasenfratz and F. Niedermayer, Nucl. Phys. B414 (1994) 785; P. Hasenfratz, Nucl. Phys. B (Proc. Suppl) 34 (1994) 3; F. Niedermayer, *ibid.*, 513. A. Farchioni, P. Hasenfratz, F. Niedermayer and A. Papa, Nucl. Phys. **B454** (1995) 638.
39. T. DeGrand,A. Hasenfratz, P. Hasenfratz, F. Niedermayer, Nucl. Phys. **B454** (1995) 587, Nucl. Phys. **B454** (1995) 615.
40. T. DeGrand, A. Hasenfratz, D. Zhu, COLO-HEP-369, hep-lat/9603015.
41. U.-J. Wiese, Phys. Lett. B315 (1993) 417 , W. Bietenholz, E. Focht and U.-J. Wiese, Nucl. Phys. B436 (1995) 385, W. Bietenholz and U.-J. Wiese, MIT preprint, CTP 2423 (1995).
42. D. Bliss et al., hep-lat/9605041
43. C. Davies et al., Phys. Rev. D52 (1995) 6519, Phys. Lett.B 345 (1995) 42; Phys. Rev. D50 (1994) 6963; Phys. Rev. Lett. 73 (1994) 2654; and G.P. Lepage et al., Phys. Rev. D46 (1992) 4052.
44. M. Alford, T. Klassen and P. Lepage, presentations at Lattice 95, hep-lat/9509087, and in Lattice 96, hep-lat/9608113.

45. UKQCD collaboration, presentation at Lattice 96, hep-lat/9608034.
46. S. Collins, R. Edwards, U. Heller and J. Sloan, presentation at Lattice 96, hep-lat/9608021.
47. For a review of the experimental situation, see W. Toki, in the Proceedings of the 1996 Slac Summer Institute.
48. G. Bhanot and M. Creutz, Phys. Rev. D24, 3212 (1981); for recent work, see U. Heller, Phys. Lett. B362, 123 (1995) (hep-lat/9508009).
49. C. Morningstar and M. Peardon, contribution to Lattice 96, hep-lat/9608050.
50. R. Sommer, Nucl. Phys. B411 (1994) 839.
51. T. Schäfer and E. Shuryak, Phys. Rev. Lett. 75, 1707 (1995).
52. G. Bali, et al., Phys. Lett. B309, 378 (1993)
53. H. Chen, J. Sexton, A. Vaccarino and D. Weingarten, Nucl. Phys. B (Proc. Suppl.) 34, 347 (1994).
54. J. Sexton, A. Vaccarino and D. Weingarten, Phys. Rev. Lett. 75, 4563 (1995).
55. S. Lindenbaum and R. Longacre, Phys. Lett. B274, 492 (1992).
56. W. Lee and D. Weingarten, contribution to Lattice 96, hep-lat/9608071.
57. For the UKQCD/$f_0(1500)$ picture, see F. Close and M. Teper, RAL-96-040, contribution to the 1996 International Conference on High Energy Physics, C. Amsler and F. Close, Phys. Lett. B353, 385 (1995) and Phys. Rev. D53, 295 (1996); while for the IBM/$f_J(1710)$ picture, see D. Weingarten, contribution to Lattice 96, hep-lat/9608070.
58. For one example of this idea, see M. Shifman, Int. J. Mod. Phys. A11, 3195 (1996), hep-ph/9511469.
59. L. Montonet et al., Phys. Rev. D50, 1173 (1994) and 1995 off-year partial update for the 1995 edition available on the PDG WWW pages (URL: http://pdg.lbl.gov/).
60. J. Shigemitsu, talk at Lattice 96, hep-lat/9608058.
61. P. Burrows, to appear in the proceedings of the Slac Summer Institute, 1996.
62. A. El-Khadra, G. Hockney, A. Kronfeld, and P. Mackenzie, Phys. Rev. Lett. **69** (1992) 729.
63. G. Rodrigo and A. Santamaria, Phys. Lett. **B313** (1993) 441.
64. M. Lüscher, P. Weisz, and U. Wolff, Nucl. Phys. B359, 221 (1991);
65. M. Lüscher, R. Narayanan, P. Weisz, and U. Wolff, Nucl. Phys. B384, 168 (1992); M. Lüscher, R. Sommer, U. Wolff and P. Weisz, Nucl. Phys. B389, 247 (1993); M. Lüscher, R. Sommer, P. Weisz, and U. Wolff, Nucl. Phys. B413, 491 (1994);
66. For a comparison of the two methods, see P. Weisz, in the Proceedings

of Lattice 95, hep-lat/9511017.